Available online at www.sciencedirect.com
SCIENCE DIRECT
Tectonophysics 416 (2006) 53–79
TECTONOPHYSICS
www.elsevier.com/locate/tecto

The heterogeneous upper mantle low velocity zone

Hans Thybo

Geological Institute, University of Copenhagen, Øster Voldgade 10, DK-1350 Copenhagen K, Denmark

Accepted 28 November 2005
Available online 6 March 2006

Abstract

The upper mantle low velocity zone (LVZ) is a depth interval with slightly reduced seismic velocity compared to the surrounding depth intervals. The zone is present below a relatively constant depth of 100 km in most continental parts of the world, both in cratonic areas with high average velocity and tectonically active areas with low average velocity. Evidence for the low velocity zone arises from controlled and natural source seismology, including studies of surface waves and of primary and multiple reflections of body waves from the bounding interfaces, calculations of receiver functions, and absolute velocity tomography. The available data indicates a more pronounced reduction in seismic velocity and Q-value for S-waves than P-waves as well as high electrical conductivity in the LVZ. Seismic waves are strongly scattered by the zone, which demonstrates the existence of small-scale heterogeneity. The depth to the base of the LVZ is systematically shallower in cold, stable cratonic areas than in hot, active regions of the world. Because of its global occurrence below a relative constant depth of 100 km, the LVZ cannot be explained by metamorphic or compositional variation and rheological changes. Calculated upper mantle temperatures indicate that the rocks are close to the solidus in an interval with variable thickness below 100 km depth, provided that the rocks contain water and carbon dioxide. The presence of, even small amounts of such fluids in the mantle rocks will lower the solidus by several hundred degrees and introduce a characteristic kink on the solidus curve around 80–100 km depth. The seismic velocities and Q-values are significantly reduced of rocks, which are close to the solidus or contain small amounts of partial melt. Hence, the LVZ may be explained by upper mantle temperatures being close to the solidus in a depth interval below 100 km. Assuming that the rocks contain only limited amounts of fluids, this mechanism may explain the low velocities, Q-values, and resistivity, as well as the intrinsic scattering, and the characteristic variation in thickness of the low velocity zone.

Keywords: Mantle; Seismic velocity; Low velocity zone; Scattering; Attenuation; 8° discontinuity; Lehmann discontinuity

1. Introduction

The existence and potential causes of the upper mantle low velocity zone (LVZ) have been debated during most of the latter half of the last century. It was proposed as a general feature of the Earth's mantle in the fifties by Gutenberg who interpreted "a shadow zone caused by an LVZ centred at 100–150 km depth" (Anderson, 1989). About the same time, Lehmann (1961, 1964) proposed the existence of a general discontinuity in the upper mantle, the Lehmann Discontinuity, at a depth of ca. 220 km based on data from North America and Europe. It appears that there was a strong discussion in the sixties whether one or the other model was correct. Later studies of long-range explosion seismic profiles provided evidence for several intermixed high- and low-velocity layers in the lithospheric mantle (e.g. Ansorge and Mueller, 1973;

E-mail address: thybo@geol.ku.dk.

0040-1951/$ - see front matter © 2005 Elsevier B.V. All rights reserved.
doi:10.1016/j.tecto.2005.11.021

Hirn et al., 1973), which directed attention away from the possible existence of a general LVZ below a relatively constant depth of 100 km.

Low velocity zones may be caused by the existence of partial melt. As such it is expected that the rheologically weak zone, the asthenosphere, should be an LVZ. However, interpretations of surface wave data (e.g. Suhadolc et al., 1990) and also very long-range explosion seismic data (Guggisberg and Berthelsen, 1987), have shown that high seismic velocities may extend to deep levels of the continental mantle such that a thick zone of low velocity may be encountered only at depths exceeding 200–300 km in cold cratonic regions with low heat flow. This has been interpreted as evidence for the lithosphere–asthenosphere boundary (LAB).

The existence of the LVZ is still being debated, whereas the stronger main interfaces in the inner Earth are well established as concentric shells, where abrupt discontinuous changes in physical parameters take place: The Moho (Mohorovicic, 1909), the 410 km discontinuity (Jeffreys, 1936) and the 660 km discontinuity (Niazi and Anderson, 1965) marking the mantle transition zone, the Core–Mantle Boundary, which exhibits the strongest contrast in physical parameters in any part of the inner Earth, and the transition between the outer and inner core, which has been named the Lehmann discontinuity between the inner and outer core after Lehmann (1936). Compared to these main seismic boundaries in the Earth, the LVZ has very weak contrasts in seismic parameters to the surrounding intervals, and its detection requires high-resolution seismic data with a high signal-to-noise ratio.

The main advance in mantle geophysics over recent years has been in the field of seismic tomography at global, regional and local scales (e.g. Bijwaard et al., 1998). The tomographic principle has been applied to body and surface waves, and has provided spectacular images of structure in the mantle that may be directly linked to plate tectonic processes, such as subduction of young and old oceanic plates (Fukao and al., 2001) and rifting, which by some authors has been coupled to the existence of mantle plumes that originate from the Core–Mantle Boundary (Romanowicz and Gung, 2002; Montelli et al., 2004). The tomographic images are usually derived and displayed as perturbations from a background velocity structure, which has to be close to the average structure of the study area. The background structures are therefore based on the average structure of the Earth, e.g. on a model of the Earth, which consists of

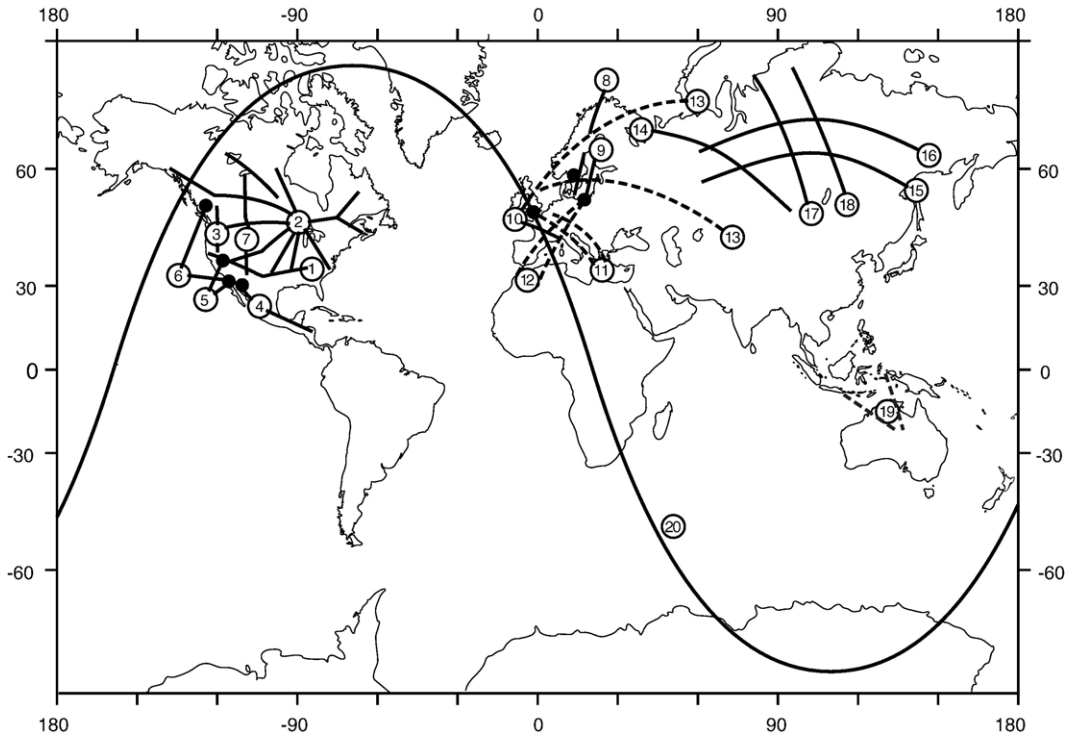

Fig. 1. Location of the high-resolution seismic profiles, which were recorded to sufficient offset to show the existence of the upper mantle low velocity zone. Numbers refer to the lines listed in Table 1. The profile line of the tomographic model in Fig. 10 (No. 20) is also shown.

concentric layers, each with uniform physical parameters. Usually the tomographic images show perturbations of the order of up to 2–3% from the background model, whereas the contrasts at the main interfaces in the Earth are up to 40%. These discontinuities, therefore, display much larger contrasts than the perturbations related to structure obtained from mantle tomography. As such, better constraints on these main interfaces in the Earth may provide new knowledge of processes in the Earth's interior, and it may be timely again to focus on these significant boundaries.

The LVZ is bounded by two interfaces: the top has been named the 8° discontinuity (Thybo and Perchuc, 1997) or the Hales discontinuity (Hales, 1991), and the base, which, as I will argue, corresponds to the upper mantle Lehmann discontinuity (Lehmann, 1961, 1964). Recent research has provided much new evidence for the existence of the LVZ as well as for the variation in physical parameters in the zone and the variation in depth to its base. This paper reviews these findings with focus on the seismological evidence from travel time and amplitude studies, as well as on the physical–chemical origin of the observed structure. The available data show that the LVZ appears globally at an approximately constant depth of 100±20 km, but nevertheless the absolute seismic velocity of the zone differs between regions, c.f. the global distribution of high-resolution seismic profiles (Fig. 1) that are recorded to sufficient offset to show evidence of the feature. The LVZ is identified in cratonic areas with high average seismic velocity in the upper mantle; in such areas the absolute velocity of the LVZ is higher than the global average but lower than in the surrounding depth intervals. It is also identified in tectonically active areas with small average mantle velocity, where the velocity of the LVZ is also small and smaller than in the surrounding intervals.

2. Observations of the upper mantle low velocity zone

Depth intervals with lower seismic velocity than the surrounding zones in the Earth are difficult to identify and interpret for their seismic parameters based on surface observations of seismic body waves, because the seismic energy will not propagate horizontally in the zone, unless structure or scattering facilitate such propagation (Hill and Levander, 1984). In body wave seismology, low velocity zones are usually identified from a lateral termination of the propagation of certain seismic phases. However, such termination may also be caused by structural changes in the Earth, which makes unique identification of the low velocity zone impossible if the interpretation is based on only the record section from a single shot point. Nevertheless, the same type of termination of seismic phases has been identified at approximately the same offset of ca. 8° in all existing long-range, high-resolution seismic sections from a global compilation (Thybo and Perchuc, 1997). Although such termination could in principle be caused by structure in the Earth, we notice that the same phenomenon has been observed at approximately the same offset of 800–1000 km (8°) from the seismic source in all the available sections, now totalling more than 50 sections from various regions of the globe (Fig. 1). It is very unlikely, although possible, that such a phenomenon may take place at the same offset from about 50 seismic sources distributed over the globe. However, the same observation is also made on all the sections from experiments with data acquisition along fixed linear arrays for several seismic sources distributed along the line. In these cases, the same observation is made in both directions along the line for all the shot points located within the array of seismographs. This basic observation cannot be explained by lateral, structural variation along the line, and requires vertical variation in seismic velocity and a seismic low velocity zone. The almost constant offset (800–1000 km, depending on the study area) of the termination from the seismic sources shows that reduced velocities are encountered at an approximately constant depth of ca. 100 km in all the profiles. Examples of such observation scheme include the FENNOLORA project in Scandinavia (e.g. Guggisberg and Berthelsen, 1987; Perchuc and Thybo, 1996), several profiles in Siberia where "Peaceful Nuclear Explosions" (PNE) were used as seismic source (Nielsen et al., 1999; Sultanov et al., 1999), the Deep Probe experiment (e.g. Henstock and Levander, 1998; Gorman et al., 2002), and the seismic sections from the Early Rise experiment in North America (Iyer et al., 1969; Thybo et al., 2000), where the seismic profile lines radiate in 9 directions away from a common shot point in Lake Superior.

A compilation of the available published travel times as read from long-range seismic sections (Fig. 2A) shows a characteristic division of the average velocities of seismic waves in the Earth: fast propagation in stable cratonic areas, characterised by low heat flow, and slow propagation in tectonically active areas with high heat flow (Fig. 2). Travel times for stable areas are found in an interval about 3 s wide with an average slope that indicates a large average velocity of ca. 8.4 km/s to 1300 km offset, where the slope changes to a higher velocity.

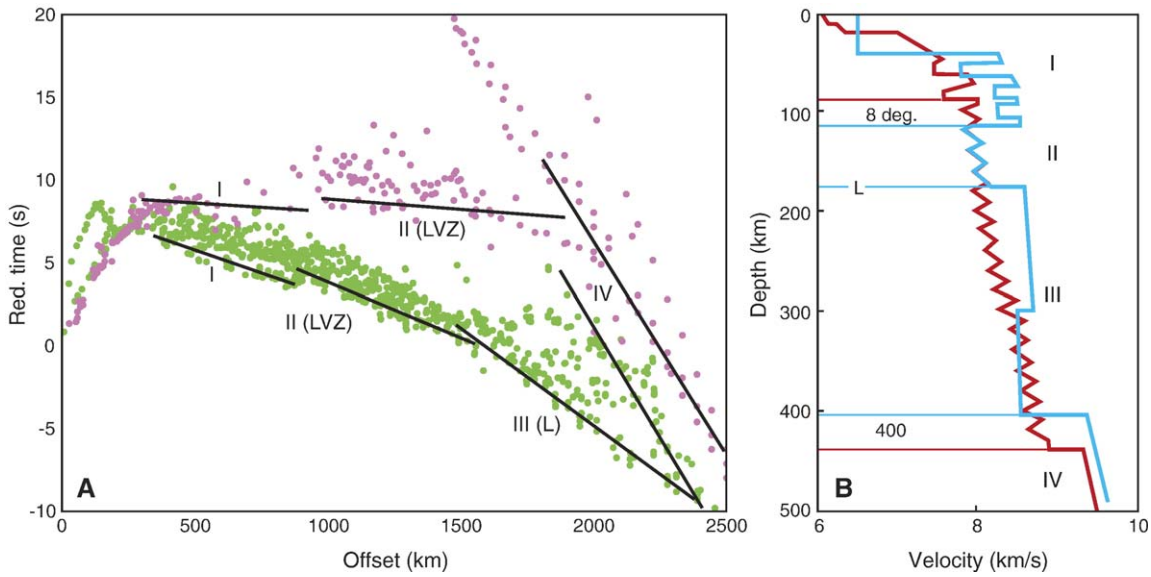

Fig. 2. Plot of a collection of published travel times (A) for long-range seismic data for hot, tectonically active (purple points) and cold, tectonically quiet areas (green points). Travel times are reduced by 8 km/s. Lines illustrate the onset of the energy and refer to: (I) uppermost mantle with linear, shingled arrivals, (II) scattered arrivals from the LVZ, (III) linear arrival from the Lehmann discontinuity, (IV) phases from the 410 km discontinuity. Notice the abrupt delay in frontal arrival times at 800–900 km offset for both cold and hot areas. (B) Representative model of the velocity–depth relation in cold (blue) and hot (red) areas. The LVZ is present in both types of region below ca. 100 km depth. It is thin in cold areas and thick in hot areas, where it may reach as deep as to the 410 km discontinuity.

Travel times for active areas show more scatter and the average slope indicates a much lower apparent velocity of around 8.0 km/s to almost 2000 km offset than for stable, cold areas. The difference in seismic travel times between the two groups of arrivals is 7–8 s at 1800 km offset from the source. Close inspection of the two clusters of travel times shows that there is a delay of 0.5–1.0 s at around 800–900 km offset (marked by 8°). The number of points is highest for the stable areas, such that the delay is most clearly expressed for this cluster, but it may also be identified in active regions. This delay demonstrates the existence of a general low velocity zone (LVZ) below the 8° discontinuity at ca. 100 km depth in the upper mantle. The average travel time for active regions extends to very large offsets of ca. 2000 km where the phases from the transition zone take over as first arrivals. This is different for stable areas where there is a change of slope of the average curve at ca. 1300 km offset to a delayed linear phase with higher velocity (marked L), which is the expression of the base of the LVZ. This seismic phase corresponds also to the original definition of the upper mantle Lehmann discontinuity (Lehmann, 1961, 1964), which hereby is being interpreted as the base of the LVZ. The variability in the offset to the onset of the Lehmann phase corresponds to variation in the depth to the base of the LVZ. The two characteristic velocity depth profiles (Fig. 2B) illustrate the above analysis of travel times. The velocity profile for stable areas shows a low velocity zone below a depth of 100 km with a distinct change to higher velocity at its base. The low velocity zone for active areas extends deep into the upper mantle, perhaps to the top of the transition zone at some locations. The sharp undulations on the two profiles illustrate that we interpret strong scattering from the interval below 100 km depth in the seismic sections.

In the following part, I present a series of examples of such observations in several types of seismic high-resolution data, some of which are only available as paper prints of the sections, and some as digital data, which can be subject to modern processing techniques. There is a shortage of controlled source data acquired to sufficient offset later than 1990, and therefore, all the available digital data has been digitized from recordings on analogue tapes with the exception of the Deep Probe data, which was acquired in the 90's (Henstock and Levander, 1998). Several data sets are only available as printed seismic record sections, and digital processing of this data cannot be carried out. Nevertheless, all the available long-range, high-density record sections that extend to sufficient offset are of sufficient quality to show a characteristic delay of the first arrival at around 800 km offset from the source as well as a long coda behind the first arrival in the offset range of ca. 500–

1400 km. The delay at 800 km offset follows smaller delays at shorter offsets, where the first arrivals appear as short sections of shingled linear phases, indicative of a series of intermixed high- and low-velocity layers in the upper mantle down to the LVZ.

In all the seismic sections listed in Table 1 we observe a series of general features:

1. A pronounced delay of the first arrival phase at 800–1000 km offset, which demonstrates that an LVZ must exist below the 8° discontinuity at 100 km depth.
2. Highly variable arrival times of the first arrival between the delay at ~8° offset and a characteristic offset x_L for the region in concern.
3. Beyond this characteristic offset x_L, the first arrival again appears as a coherent seismic phase in all cratonic areas (the delayed linear phase corresponding to the Lehmann phase).
4. A pronounced coda behind the first arrival in the offset interval of ~500–1400 km. It appears close to the first arrival at far offset and with significant delay at short offset. It has long duration at short offset and shorter duration at far offset. This coda indicates the existence of small scale heterogeneity in the LVZ.

In the following, a series of examples of these features is illustrated by seismic data from various seismic projects around the world.

The FENNOLORA experiment was carried out in 1979 as a seismic long-range project along a profile line through Scandinavia between the North Cape and Poland based on 9 strong seismic sources from detonation of chemical explosives. Data acquisition was carried out with analogue MARS-66 mobile seismographs and the data was subsequently digitized from the analogue, frequency-modulated tapes. The seismic sections are of high quality with a nominal distance between seismic traces of ca. 15 km for most shot points, and they show clear P- and S-wave arrivals. Seven of the seismic sections have been recorded to offsets far enough to show the termination of the first arrival at around 8° offset.

Shot point I was detonated in the Atlantic Ocean to the north of the North Cape. The data shows energy out to the farthest recorded offset of more than 2500 km at stations in southern Sweden. The seismic record sections clearly show the characteristic features of the LVZ with $x_L = 1200$ km (Fig. 3). The observations at far offset are only made in the P-wave section, because the S-wave section looses its energy from about 1100 km offset, indicative of exceptionally strong attenuation of the S-waves in the LVZ. The delay from the LVZ is more pronounced for S-waves than P-waves, indicative of a stronger reduction in S- than P-wave velocity.

The other seven long-range sections from the FENNOLORA experiment qualitatively all show the same characteristic features (c.f. Perchuc and Thybo,

Table 1
List of seismic, high-resolution lines with sufficient length to show the existence of the upper mantle low velocity zone, together with the profile line (No. 20) of the tomographic model in Fig. 10

Number	Region	Project name	Source type	Model type	Author
1	N. America	GNOME	Nuclear explosion	Hot & cold	Romney et al. (1962)
2	N. America	Early Rise	Chemical explosion	Hot & cold	Warren et al. (1968), Iyer et al. (1969)
3	N. America	Na	Chemical explosion	Hot	Hill (1972)
4	N. America	SCARLET	Earthquakes	Hot	Walck (1984)
5	N. America	PAC-NW	Chemical explosion	Hot	Miller et al. (1997)
6	N. America	Na	Nuclear explosion.	Hot & cold	Vidale et al. (1995)
7	N. America	Deep Probe	Chemical explosion	Cold	Henstock and Levander (1998)
8	Scandinavia	FENNOLORA	Chemical explosion	Cold	Hauser et al. (1990)
9	Scandinavia	BABEL	Airgun	Cold	BABEL Working Group (1991)
10	Hot & cold	Brest	Chemical explosion	Intermediate	Hirn et al. (1973)
11	Europe	Na	Earthquakes	Intermediate	Mayer and Mueller (1973)
12	Europe	Na	Earthquakes	Intermediate	Mayer and Mueller (1973)
13	Eurasia	Na	Earthquakes	Cold	Given and Helmberger (1980)
14	Eurasia	Quartz	Nuclear explosion	Cold	Mechie et al. (1993), Morozova et al. (2000)
15	Siberia	Kimberlite	Nuclear explosion	Cold	Fuchs (1997)
16	Siberia	Craton	Nuclear explosion	Cold	Nielsen et al. (2002)
17	Siberia	Meteorite	Nuclear explosion	Cold	Fuchs (1997)
18	Siberia	Rift	Nuclear explosion	Cold	Priestley et al. (1994)
19	Australia	Skippy	Earthquakes	Hot & cold	Bowman and Kennett (1990)
20			Earthquakes		Zhang and Tanimoto (1993)

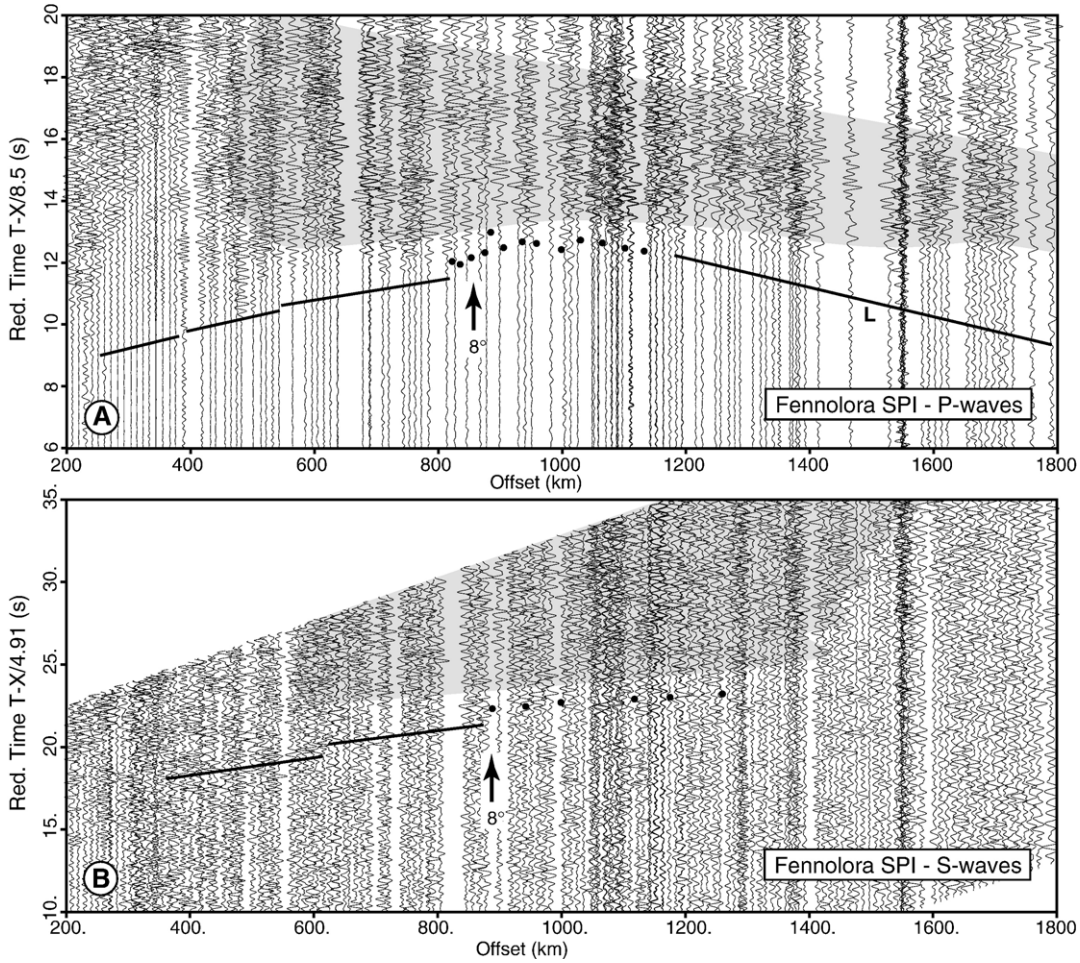

Fig. 3. Seismic record sections from the FENNOLORA project for the northernmost shot point I at the North Cape recorded in Norway and Sweden (profile 8 in Fig. 1). A) P-wave section, reduced by a velocity of 8.5 km/s; B) S-wave section reduced by a velocity of 4.91 km/s. Lines illustrate correlated phases, dots show the first arrival at the scattered arrivals from the upper mantle low velocity zone. Notice the loss of energy in the S-wave section at offsets above 1000–1200 km, i.e. for waves that have travelled in the low velocity zone. This demonstrates the strong attenuation in the LVZ of S-waves in particular. Therefore only the P-wave section shows a refracted Lehmann phase (L). The grey areas mark those parts of the seismogram sections where significant ringing or reverberations occur after the first arrival; these phases represent strong reflectivity in the mantle low velocity zone.

1996), with slight variation in the offset to the 8° delay (±50 km) and the offset x_L to the delayed linear phase (±100 km). The delayed linear phase (Lehmann arrival) generally appears at farther offsets in the southern part of Scandinavia than in the northern parts, which indicates that the LVZ extends to deeper levels in the southern than northern Baltic Shield. Similarly, variation in the offset of the characteristic 8° delay indicates that the LVZ is slightly deeper in northern (ca. 120 km deep) than in southern (100 km deep) Scandinavia (Perchuc and Thybo, 1996). This interpretation is based on observations of the characteristic features in both directions in all the record sections that were recorded to offsets larger than 1000 km. The delay cannot be explained only by lateral variation in seismic velocity and requires a seismic low velocity zone below a depth of 100–120 km, which is thicker in southern than in northern Scandinavia, and which is highly heterogeneous.

The coda to the first arrival is observed in the offset range of about 500 to 1500–1800 km with more than 7 s duration at short offset and of the order of more than 2–3 s at far offsets. A long-range seismic section from the EUGENO-S experiment in the southern part of the Baltic Shield shows the same general features as the FENNOLORA sections (Perchuc and Thybo, 1996), although the section is relatively short and, therefore, cannot show the delayed, linear first arrival

at far offsets. A documentation of the FENNOLORA data set by a series of plots of the record sections (Hauser et al., 1990) provides further documentation of the above observations.

The BABEL (Baltic and Bothnian Echoes from the Lithosphere) project recorded seismic waves from airgun detonations at sea on an array of onshore stations distributed over the Nordic countries around the Baltic and Bothnian Seas. Particular successful registration took place on the southern part of the island of Öland in the southern Baltic Sea to the east of onshore Sweden. By use of stacking of multi-channel registrations at 75 m intervals, a record section from this station shows seismic arrivals to offsets of around 700 km at trace intervals of 1 km (BABEL Working Group, 1991; Fig. 4). In the offset interval of 550–700 km the record section shows a series of strong seismic arrivals, which occur at "random times" between 5 and 7 s reduced time with a reduction velocity of 8 km/s. These strong arrivals appear as linear events with individual lengths of less than 10 km. Several similar arrivals are observed as uncorrelated energy behind the first, strong arrivals. This coda indicates seismic reflections from a heterogeneous medium with scattered reflectors of individual lengths of less than 5 km from the interval below 100 km in the upper mantle. The maximum length of the arrivals (10 km) is below the size of the Fresnel Zone at the applied frequency band, such that it is uncertain whether they originate from separate reflectors or are caused by constructive interference between a series of seismic phases from the same depth interval. The station at southern Öland was located close to the position of shot point B of the FENNOLORA project, for which registrations were done onshore, close to the detonations of the airguns. The record section for shot point B shows features which are similar to the observations made in the same offset interval on the airgun section (Fig. 4). The strongest arrivals are also scattered and appear at reduced times of 6.0–7.5 s. They are followed by a strong coda of more than 4 s duration. The lateral sampling interval of the section is coarser than the airgun section, such that details cannot be observed in

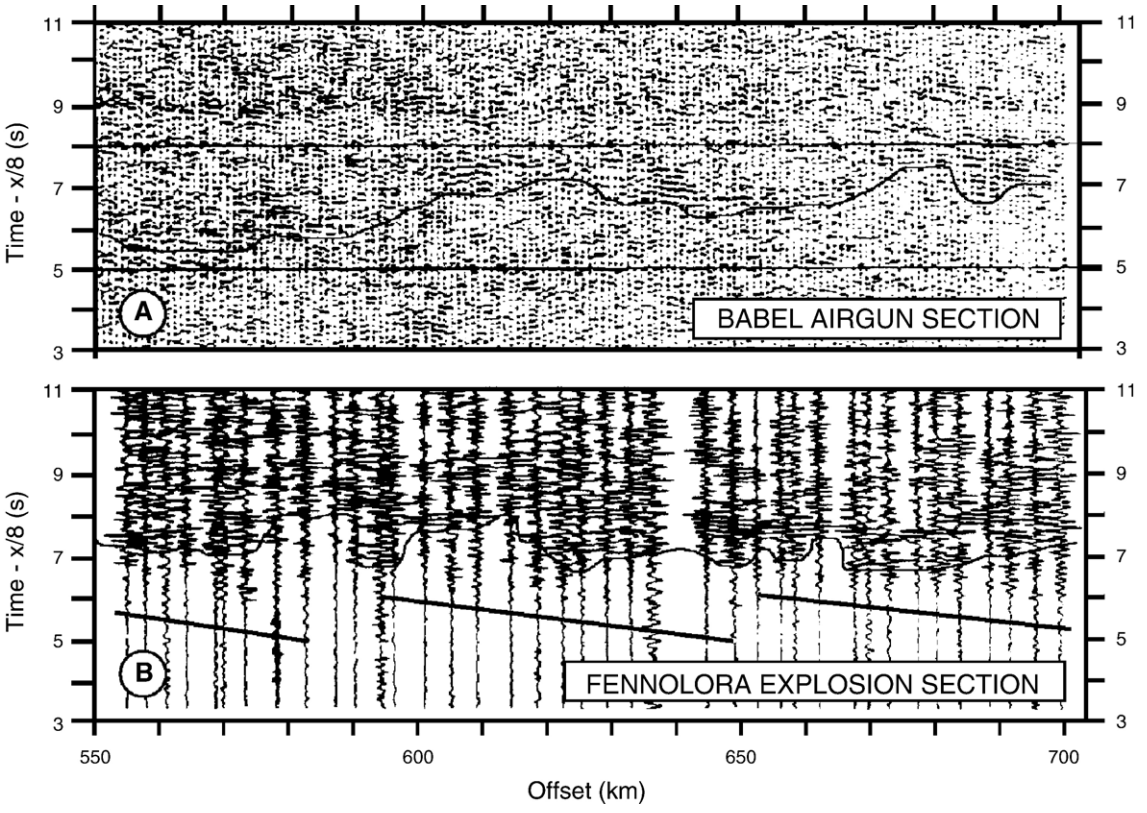

Fig. 4. Details of the scattered waves from the low velocity zone, illustrated by seismic data from the BABEL project (A: profile 9 in Fig. 1) and the FENNOLORA project (B: profile 8 in Fig. 1). The upper panel is based on stacked airgun data with a recording interval of 75 m to a seismogram interval of 1 km. Notice the scattered arrivals with lengths of less than 10 km, i.e. smaller than the width of the Fresnel zone. The lower panel is based on onshore recordings of seismic waves from chemical explosions. Notice how the scattered arrivals appear random at this scale and that the first arrival can be observed with this data (shown by linear lines).

the scattered wave field. However, the explosion section shows that the first arrivals are much weaker and arrive earlier than the strong arrivals as a series of en-echelon linear arrivals between 5 and 6 s. These first arrivals are probably too weak to be detected by the airgun section.

The Early Rise long-range experiment was carried out in North America in the mid sixties. Data was acquired along nine profiles for a series of large explosions in Lake Superior. The profiles all radiate away from the shot point and cover the whole azimuthal range (Fig. 1). In principle, such a configuration enables studies of the overall mantle anisotropy. Analysis of all the published record sections from this experiment confirms the existence of the characteristic delay at around 8° offset in all directions from the shot location (Fig. 5) at almost the same offset for all the record sections (±50 km), indicative of only slight azimuthal variation in the depth to the LVZ around the shot point in Lake Superior. The far offset, delayed linear arrival (Lehmann arrival) is observed, but at shorter offsets than in the FENNOLORA data from Scandinavia (between 1100 and 1300 km, depending on the azimuth). This indicates that the LVZ is thinner in most parts of the central North American craton than in Scandinavia. The shortest offset to the Lehmann arrival is observed on the profiles that extend to the northwest into the Canadian Shield. Fig. 5 further illustrates the existence of a coda, more than 5 s long with high amplitude from ca. 1 s after the first arrival. This section further shows much stronger scattering of the first arrival at offsets beyond ca. 1400 km. This scattering has been explained (Thybo et al., 2000) as the result of the transition from cratonic North America to the active, western part with a thick LVZ.

An invaluable set of high-resolution seismic recordings has been acquired in the former Soviet Union. During the period 1965–88, Russian seismologists were able to use nuclear explosions as sources for seismic recordings along a network of profiles, primarily in Siberia. These seismic sources were powerful enough to allow registration on arrays of mobile seismographs to beyond 4000 km offset and even registrations of seismic reflections from the Core–Mantle Boundary (Thybo et al., 2003a). Registrations were generally carried out with 15–20 km station spacing along the profile lines. As a typical example of the PNE data set, the record section from Kimberlite shot point 3 (Fig. 6) shows a clear delay of the first arrival at 800–850 km offset and a pronounced coda, extending for at least 5 s after the first arrival. The delayed, linear first arrival at far offsets is similarly observed in all record sections of the Soviet Russian programme. Much of the extensive data set has been the subject of intense analyses by western scientists since it became available in the early 1990's after a German–Russian collaboration on digitization of the original analogue tapes (e.g. Mechie et al., 1993; Thybo and Perchuc, 1997; Fuchs, 1997; Nielsen et al., 1999; Ryberg and Wenzel, 1999; Morozova et al., 2000;

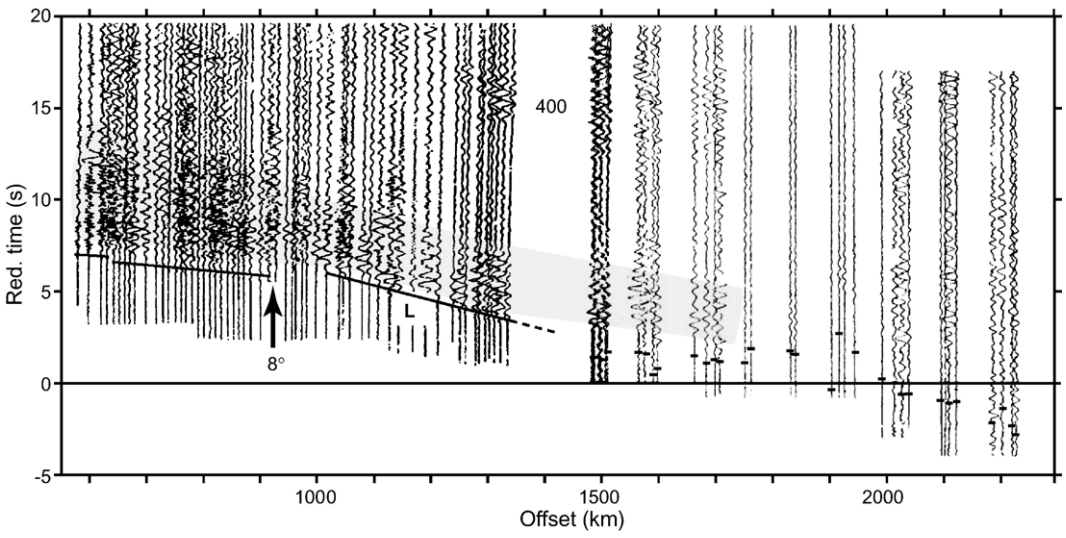

Fig. 5. A composite record section from Early Rise profiles 8 and 9 (the line between 2 and 3 in Fig. 1) acquired for the shot point in Lake Superior. The section shows clear linear first arrivals at offsets below 800–900 km and a clear Lehmann refraction arrival at offsets beyond 1050–1100 km. In between we observe the travel time delay and the random arrivals from the low velocity zone. Behind the first arrivals a significant coda of 5–7 s duration is observed, indicative of the scattering from the LVZ. The scattered arrivals beyond 1400–1500 km offset are due to the lateral transition from cratonic to tectonically active North America.

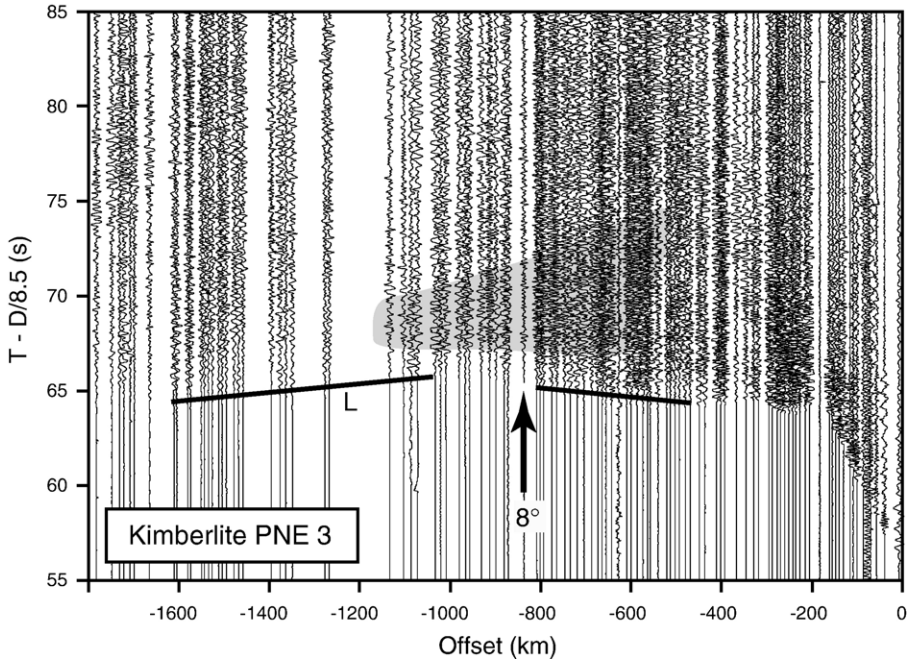

Fig. 6. Seismic record section based on recordings of waves from Kimberlite shot point 3 in Siberia (profile 15 in Fig. 1). Notice the change in appearance of the first arrival at 850 and 1150 km offset between linear arrivals and scattered arrivals from the low velocity zone. The grey area illustrates the coda of scattered energy from the LVZ. The grey areas mark those parts of the seismogram sections where significant ringing or reverberations occur after the first arrival; these phases represent strong reflectivity in the mantle low velocity zone.

Nielsen et al., 2002; Nielsen and Thybo, 2003). Our analysis has shown that all the available data from this large programme shows evidence for the characteristic delay from the LVZ, the coda, and the far offset, delayed linear arrival with small variation in the exact offsets (±75 km, resp. ±100 km) and duration of the coda (±2 s).

The only recent explosion seismic experiment for investigation of the Earth's mantle is the Deep Probe experiment (Henstock and Levander, 1998; Gorman et al., 2002). This data was acquired with a very dense spacing between the seismographs along a NS trending profile in the Rocky Mountains between central Canada and southern US. The seismic sections from this experiment show the basic characteristics for the LVZ (Fig. 7), including the pronounced delay, an up to 7 s long coda and the delayed linear phase from the Lehmann discontinuity.

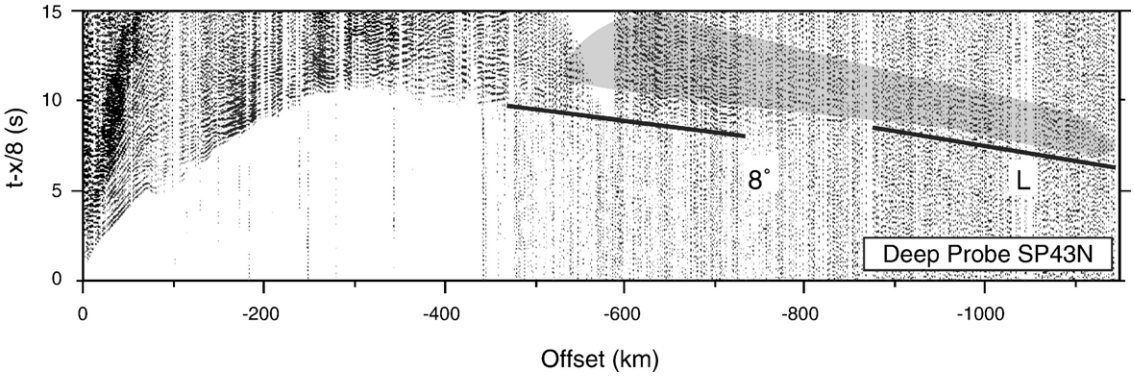

Fig. 7. Seismic section from the Deep Probe project in North America (Henstock and Levander, 1998) for shot point 43 recorded northwards (profile 7 in Fig. 1). The section shows clear evidence for the 8° delay at ca. 800 km offset and the delayed, linear phase (Lehmann refraction) from around 900 km offset, indicative of a thin LVZ in this part of Canada. The grey areas mark those parts of the seismogram sections where significant ringing or reverberations occur after the first arrival; these phases represent strong reflectivity in the mantle low velocity zone.

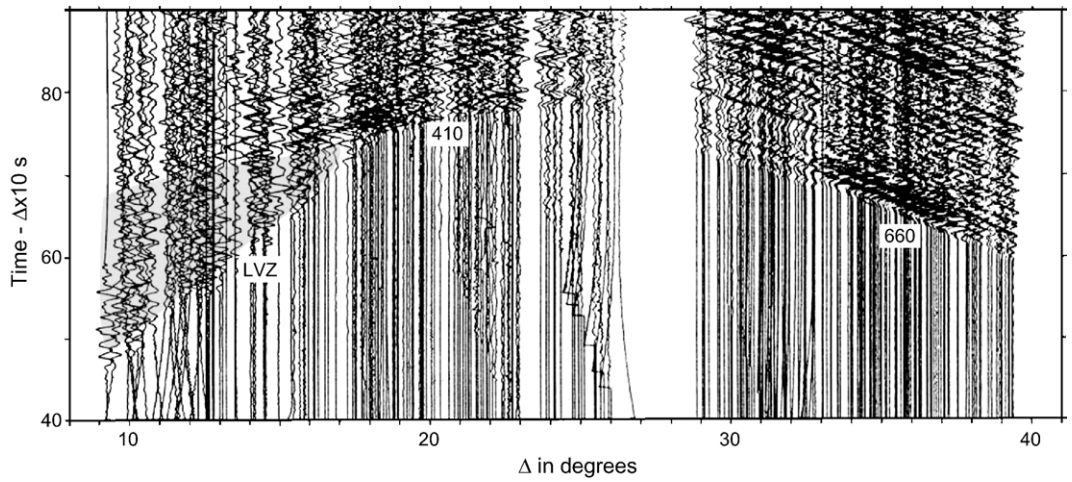

Fig. 8. Seismic record section from the SCARLET project in western North America (Walck, 1984) based on recordings on arrays in California of seismic waves from earthquakes in Baja California (marked by No. 4 in Fig. 1). The section illustrates how the scattered first arrivals with small apparent velocity continue to far offsets, out to the arrivals from the 410 km discontinuity, i.e. the LVZ must extend downwards to near the mantle transition zone.

Most of the available long-range seismic sections to offsets far enough to show the delay from the LVZ have been acquired in tectonically stable regions, i.e. in cratonic areas. Observation of the characteristic features of the LVZ requires a profile length of more than 1000 km, which is often difficult to achieve in tectonically active regions. Only very few examples exist from the active areas of the Earth. One particular example is from western North America, acquired on seismological arrays in California for earthquakes in Baja California (Walck, 1984). This section (Fig. 8) indicates that the LVZ extends very deep in this area, probably to depths close to the top of the mantle transition zone as modelled by Thybo and Perchuc (1997). The average velocity is very small (8.35 km/s) out to the cross-over with the 410-phase and the first arrivals appear scattered compared to the linear arrivals from the transition zone, indicative of scattering from the upper mantle above the transition zone.

3. Seismic velocity models from travel time modelling

Application of ray tracing modelling and inversion of seismic travel times from explosion seismic data provides details of the distribution of seismic velocity in the lithosphere. Usually such methods are restricted to 2 dimensions, mainly because the demand for dense registrations implies limitations to data acquisition along profile lines, for data to be sampled at sufficient density for obtaining high-resolution. Several high-density data sets along individual profiles to very large offset have recently been modelled for the velocity distribution in the crust and upper mantle.

The FENNOLORA project acquired one of the first long-range explosion seismic data sets along a north–south striking profile in Scandinavia with offsets large enough to allow detailed modelling of upper mantle structure down to depths of 400 km. Guggisberg and Berthelsen (1987) and Guggisberg et al. (1991) interpret the depth variation to the lithosphere–asthenosphere boundary along the profile from ca. 100 km in the southern part to more than 250 km in the northern part of Scandinavia. The lithosphere was shown to include a series of intermixed high- and low-velocity layers. Stangl (1990) based his reinterpretation of both P- and S-wave velocity on a more detailed model of Moho depth and velocity variation in the crust than Guggisberg et al. (1991). His models are based on travel time picks of first and secondary refracted and reflected P- and S-waves from the 9 shots along the more than 2000 km long profile. The result includes a distinct low velocity layer along the whole profile below 100 km depth in both the P- and S-wave models. Perchuc and Thybo (1996) found a systematic deepening by ca. 20 km of the top of the LVZ together with substantial thinning (by 20–30 km) of the LVZ from the southern, Proterozoic parts to the northern, Archaean parts of the Baltic Shield. Studies of the general velocity structure of the Baltic Shield for nuclear test monitoring purposes also indicate the existence of the LVZ below the Baltic Shield (Bondar and Ryaboy, 1997). Abramovitz et al. (2002) applied an automatic tomographic inversion algorithm to travel time picks of the first P- and S-wave

arrivals along the FENNOLORA profile. Identification of first arrivals is a very reliable process, and the uncertainty of the picks is small, usually 100–200 ms for P- and 200–400 ms for S-waves. The results show the existence of the LVZ in the depth range of ca. 100–150 km along the whole profile as a zone with negative vertical gradient. The ratio between P- and S-wave velocities is higher in the LVZ than in the surrounding depth intervals, thus confirming the independent results of Stangl (1990) that the Poisson's ratio is high in this zone. Abramovitz et al. (2002) further present evidence for extremely strong attenuation of the S-waves in the LVZ (c.f. also Fig. 3).

Recently, several interpretations have been published based on travel time modelling of parts of the Peaceful Nuclear Explosion (PNE) database. Ryberg et al. (1996) present an interpretation of seismic P-wave velocity along the QUARZ profile between the White Sea and southern Siberian Russia (profile 14 in Fig. 1) where delays in the travel time curves indicate the presence of the LVZ. A later interpretation of the same data set by Morozova et al. (2000) with better crustal control confirm this result with the LVZ being situated between 120–140 and 170 km, thickest below the central part of the profile. These authors further model the Q-factor in the various layers of this model and find evidence for very strong attenuation, with Q=400 in the LVZ, compared to Q-values of 700–1300 in the surrounding depth levels (Morozov et al., 1998a). Travel time and waveform modelling with 1D models, based on application of the 3D reflectivity method of the RIFT profile of the PNE programme in Siberia, indicate that a thin LVZ exists below a depth of ca. 130 km (Priestley et al., 1994). Two-dimensional ray trace modelling, including structural variation along this profile, indicates that the LVZ may be shallower and located in the depth interval of 80–90 to 110 km (Pavlenkova and Cipar, 2002). Based on amplitude modelling, the latter authors find that there is a strong velocity discontinuity at the base of the LVZ.

Tomographic velocity inversion of first arrivals along PNE profile KRATON in Siberia has shown compelling evidence for the existence of the LVZ in eastern and central Siberia (Nielsen et al., 1999). Data acquired along the 3500 km long profile for four shot points constrain the velocity distribution down to more than 400 km in the central part of the profile. The depth range around 100 km has good ray coverage along 2500 km of the profile, where the calculated model includes a zone of negative vertical velocity gradient between approximately 100 and 180 km depth. The uncertainty of the absolute depths is of the order of 20 km. The applied tomographic inversion method is based on calculation of absolute velocity, and not perturbations relative to a standard velocity–depth model, as is often the case in teleseismic tomography. The result is therefore to a large degree independent of the initial velocity model, as also tests have shown.

Early 1D-models of the Early Rise data include a pronounced LVZ between 100 and 160 km depth (Green and Hales, 1968). Later modelling of this large dataset also includes the LVZ, but with a smaller velocity contrast to the surrounding intervals (e.g. Hill, 1974; Masse et al., 1972). The LVZ is everywhere determined on the basis of a delay of first arrivals at around 8° offset from the source. Another pronounced delay is found at farther, variable offset in the seismic sections of the Early Rise project. Masse (1973) interprets this second delay on the southwesterly trending profile as evidence for the transition from a shield type of velocity structure with a thin LVZ to the velocity structure of western, tectonically active North America. A similar delay is observed in all directions away from the central shot point in Lake Superior (Thybo et al., 2000). The corresponding transitions correlate with a pronounced change in velocity structure from positive to negative S-wave perturbation in the tomographic velocity model by van der Lee and Nolet (1997). The delay may be explained by an abrupt change in velocity structure from a ca. 40 km thick to a more than 100–200 km thick LVZ, as demonstrated by two-dimensional travel time modelling (Thybo et al., 2000). The change occurs over less than 100–200 km laterally, and it is observed in all directions from the source location. This lateral transitional zone further correlates with the location of the majority of the intracratonic earthquakes in North America. Thybo et al. (2000) demonstrate that the stress induced from the density difference across this abrupt lateral zone may induce lateral flow in the mantle, which may explain the occurrence of the majority of the enigmatic intraplate earthquakes in North America.

4. Geophysical characteristics of the LVZ

4.1. Velocity variation

The LVZ has been observed in a variety of seismic data from many parts of the globe. Examples include eastern, central and western North America (e.g. Hill, 1972; Burdick, 1978; Grand and Helmberger, 1984; Thybo et al., 2000), and Eurasia (e.g. Given and Helmberger, 1980; Priestley et al., 1994; Nielsen et al., 1999; Morozova et al., 2000). These interpretations are

based on body and surface wave observations and different types of modelling techniques. Helmberger (1973) used travel time and waveform modelling of body waves observed in North America from the Nevada test site to study the LVZ in detail. He concluded that a 40–70 km thick zone of lower velocity than the surrounding intervals exists in the mantle below ca. 80 km depth. By use of similar methods Given and Helmberger (1980) conclude that there is a thin LVZ below a depth of 150 km under Eurasia. Helmberger and Engen (1974) model a pronounced LVZ in the P-wave velocity structure below a depth of ca. 100 km by use of data from permanent seismograph stations in North America. Remarkably, they find only evidence for a thin LVZ in the S-wave velocity structure, whereas Masse (1973) interprets a thick depth interval with reduced S-wave velocity but only a thin low velocity channel in the P-wave velocity structure. Hales (1991) finds evidence for a significant LVZ below large parts of North America from recordings of seismic waves from nuclear test explosions.

Body wave analysis may detect the presence of low velocity zones in the Earth's interior, but the interpreted seismic parameters based on body waves are uncertain. Surface waves are potentially better suited for determination of the seismic parameters of the LVZ, but the resolution is generally lower as the measurements average over large lateral distances. Calcagnile (1991) inverted surface wave dispersion curves for two paths across the Baltic Shield and interprets a zone of reduced P- and S-wave velocity which is thicker than 100 km. Suhadolc et al. (1990) find a depth to the LVZ of less than 100 km everywhere in central Europe, except for underneath the Alps and the Apennines. van Heijst et al. (1994) made a synthetic study of the potential of surface wave analysis for identification of low velocity zones in the upper mantle. They conclude that the zone must be thick in order to be detectable at the available frequencies. Pontevivo and Thybo (2006) extend this study by using the Hedgehog inversion technique (Knopoff, 1972; Panza, 1981), and find that the LVZ must be of the order of 80 km thick for dispersion analysis of surface waves to uniquely identify its presence for a velocity contrast of 2% to the surrounding depth intervals. If the velocity contrast is 5%, the zone only has to be 40 km thick to make it detectable. The authors invert dispersion curves for waves travelling across Siberia from seismic events around Japan. The results show that a zone with slightly reduced S-wave velocity or constant vertical gradient is present in eastern Siberia below a depth of 80 km (Fig. 9) in agreement with the results by Nielsen et al. (1999). This result also confirms the existence of the LVZ in the background model of results from surface wave tomography in Eurasia (Villasenor et al., 2001). Darbyshire (2003, 2005) presents extensive tomographic inversion of surface wave data with travel paths across large parts of Canada and the whole of Greenland, by which she identifies a distinct low-velocity zone beneath approximately 100 km depth throughout this whole area.

Global models of seismic velocity from interpretation of surface wave propagation include a low velocity zone in the depth range below 100 km. It is well established that the LVZ exists below depths of 100 km beneath the oceans and the average velocity model of the Earth (PREM) includes a low velocity zone between 100 and 220 km depth (Dziewonski and Anderson, 1981). It has been speculated that the LVZ may only be present beneath the oceans, and there is little doubt that it is most pronounced under the oceans. The IASP91 model (Kennett and Engdahl, 1991) for continental areas also includes a zone of constant velocity in this depth interval. Boschi and Ekström (2002) present models of characteristic S-wave velocity models of various regions based on global inversion of surface waves. They find compelling evidence for the LVZ in all regions, including the cold and stable cratons, e.g. the Canadian Shield, and the active regions, including the western US (Fig. 9). They further present evidence for substantial S-wave anisotropy in the upper mantle LVZ. Their results show a sharper transition from the small velocities in the LVZ to the larger velocities in the underlying medium in the cratonic areas than in the tectonically active areas. This finding indirectly confirms the presence of the Lehmann discontinuity below cratonic areas at relatively shallow depths of around 200 km, and that this discontinuity is deeper in other areas.

Seismic surface waves may be inverted for lateral variation in wave speed. The results are usually presented as relative perturbations from a reference model, which may also be the initial model for the linearised inversion. Priestley and Debayle (2003) present an Sv-wavespeed tomographic model and find that it shows a pronounced and abrupt division between high wave speed beneath the stable cratonic region of north–central Asia and low wave speed further to the east and south. They also interpret the depth to the base of the lithosphere to be between 175 and 225 km depth based on their display of velocity relative to their reference model (the smoothed PREM model), which includes a steep vertical gradient at the same depth. However, absolute velocity calculated from their model shows the existence of a low velocity channel over the

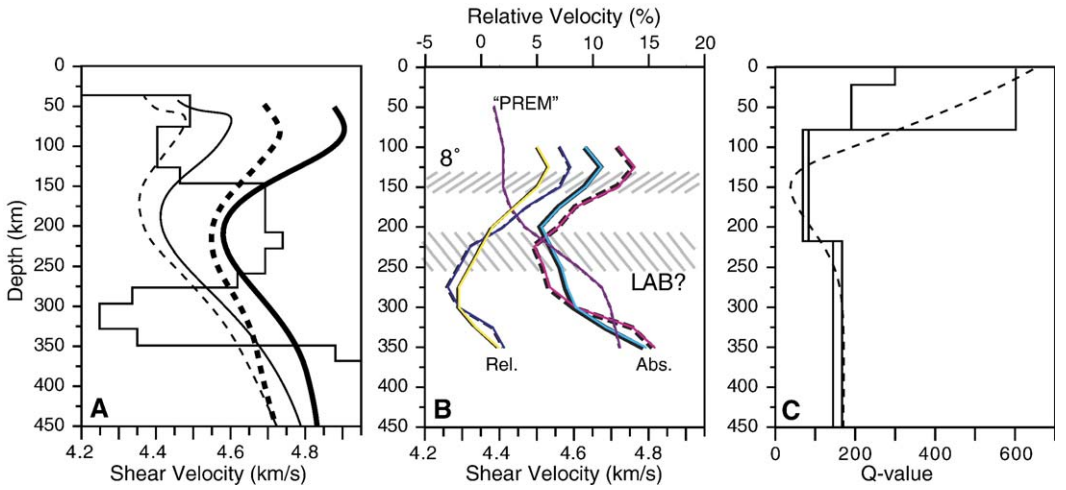

Fig. 9. Plots of seismic velocity–depth profiles from inversions of surface wave data. A) Smooth curves are typical results (Boschi and Ekström, 2002), showing a clear low velocity zone around a depth of 150 km for SV waves (stippled lines) and SH waves (full lines); data are shown for the Canadian Shield (bold lines) and western North America (normal lines). Notice the very gradual increase in velocity for western N. America, indicative of a deep reaching LVZ and the clear indication for anisotropy, also in the LVZ. The curve with sharp corners is the velocity–depth model obtained by Hedgehog inversion of surface wave data from eastern Siberia (Pontevivo and Thybo, 2006), also showing a distinct, but thin low velocity zone around a depth of 100 km inside the 250 km thick lithosphere. B) Velocity perturbations in percent (marked Rel.) relative to "smooth PREM" for Siberia (Read from tomographic model by Priestley and Debayle, 2003) and calculated absolute shear velocity (marked Abs.) for the same profiles. Notice how the relative velocity profiles indicate a lithospheric thickness of 200–250 km (marked LAB) as interpreted by Priestley and Debayle (2003), whereas the Absolute velocity profile indicates an LVZ below a depth of 125–150 km (marked 8°). The "smooth PREM" model is shown by the curve marked "PREM"; notice that this reference model has zero vertical gradient between depths of 100 and 200 km and a very steep gradient from 200 to 250 km. C) Globally averaged *Q*-values (Selby and Woodhouse, 2002; smooth curve) compared to the PREM curve (Dziewonski and Anderson, 1981; with sharp corners). Notice the very strong attenuation (*Q*-values reduced to 50% of the surrounding values) in the interval between 90 and 220 km depth.

whole Siberian craton in the depth range of 125–150 and 250–300 km with a velocity reduction of up to 5%. This result is in general agreement with the result from a global study of S-wave velocity by Boschi and Ekström (2002). The vertical resolution in both these studies is probably no better than 50 km, such that there are large uncertainties in the absolute depths. The study by Pontevivo and Thybo (2006) aims at high vertical resolution, and shows the existence of a ~70 km thick LVZ with a reduction in velocity of ~2%. This is less than the resolution in the tomographic and global studies, not least considering the equivalence between thickness and velocity anomaly for the detectability of the LVZ. We may speculate that the general thick LVZ detected by global studies of surface waves may result from constructive interference between the upper mantle LVZ and the asthenospheric low velocity layer wherever the LVZ is thinner than can be resolved by these studies.

Teleseismic tomographic results usually show no indication for a globally or regionally existing LVZ because the results are presented as perturbations from a reference model, which usually includes the LVZ or a constant velocity zone in the relevant depth interval below 100 km (such as the PREM or the IASPEI91 models). Therefore, the LVZ is often only implicitly given in the results even though it is not directly seen in the presented images, as in the reference model of Spakman et al. (1993). Teleseismic tomography is usually based on inversion of relative travel time perturbations of the seismic body waves, such that the small global or regional delay expected from the LVZ will be attributed to the wave propagation through the deeper mantle from the source to the region of interest. Therefore, regional teleseismic body wave tomography cannot detect the LVZ, although relative variation in the thickness or velocity of the LVZ across the study region may be detected. Fig. 10 shows a profile that spans around the Earth from a global teleseismic inversion of travel times of seismic body waves (Zhang and Tanimoto, 1993). It is evident that there is no sign of the LVZ in the presentation of these relative results, which mainly show the significant contrast between continental and oceanic velocity structure (Fig. 10B). However, the absolute velocities (Fig. 10C) calculated from the relative velocity perturbation and the background velocity–depth curve show the presence of a distinct LVZ along the whole profile. The LVZ is mainly developed and the velocities are mainly reduced beneath

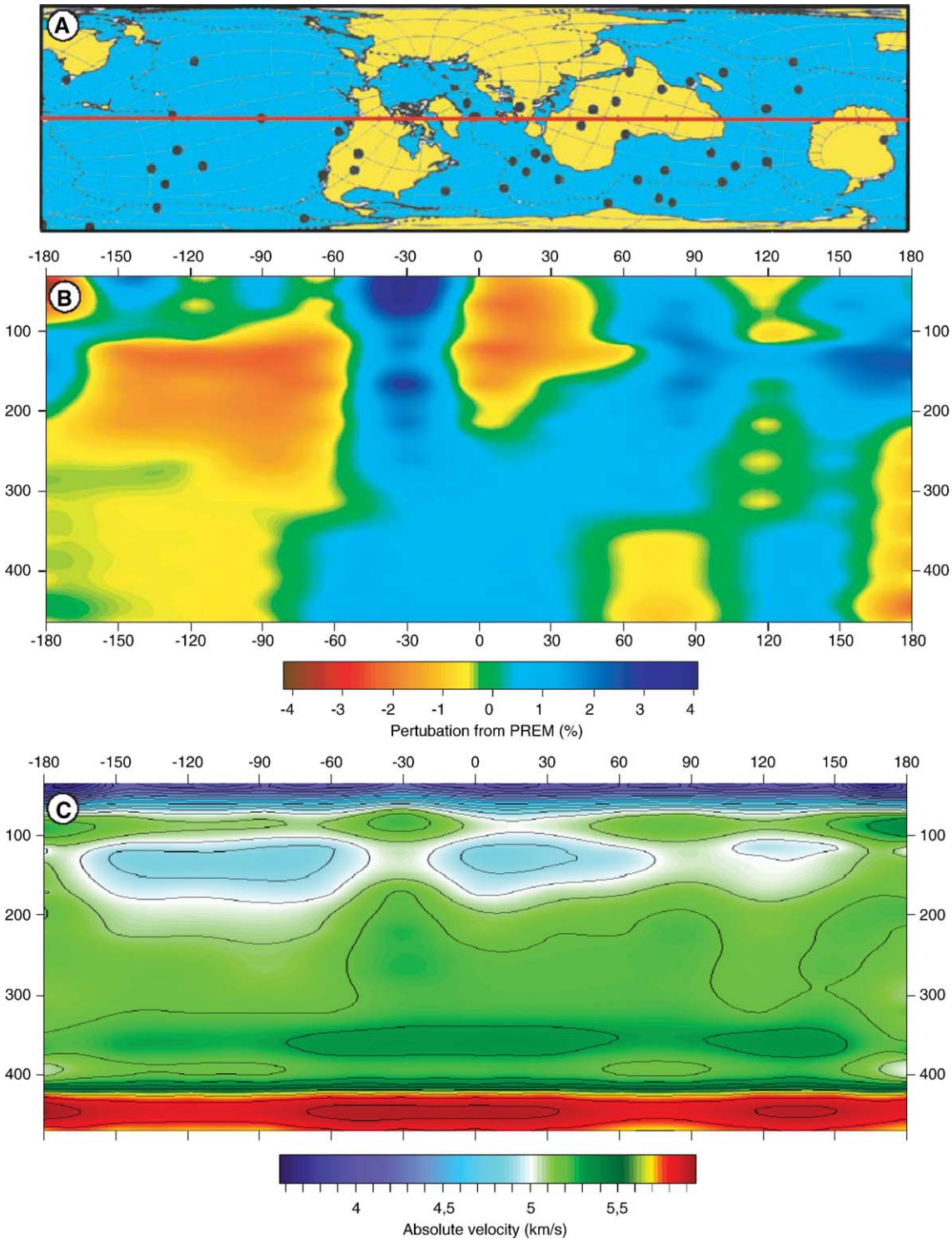

Fig. 10. The result of a global travel time inversion for seismic velocity (after Zhang and Tanimoto, 1993). A) Map of the profile, which is also illustrated in Fig. 1. B) Velocity perturbations relative to the background model, which in this case is the PREM model. This relative model does not show indication of any upper mantle low velocity zone, instead it shows abrupt changes between continents and oceans. C) Absolute velocities calculated from the perturbations and the background model. Notice how the absolute velocity model includes a pronounced, global low velocity zone, which is strongest underneath the oceans, but also clearly identifiable underneath the continents, despite the display of relative velocity perturbations does not indicate any anomaly.

the oceans, but the LVZ is also present as a thin zone below the continents with a smaller contrast in velocity to the surrounding intervals than under the oceans.

4.2. Receiver function imaging of bounding interfaces

Receiver function images of the upper mantle are often contaminated by strong surface multiples with arrival times corresponding to the expected time of conversions from the top of the low velocity zone. However, a new technique has recently been developed based on S-waves instead of P-waves. Such receiver functions are not contaminated to the same degree as conventional receiver functions by the surface multiples, which often mask for the primary signal by interference phenomena. The first results from application of this technique demonstrate the presence of a distinct seismic converter at depths between 80 and 120 km in the whole of the North Atlantic area, including Greenland and Iceland (Kumar et al., 2005). This new technique has, so far, not been applied to other continental areas.

4.3. Seismic attenuation in the LVZ

The results of studies of seismic attenuation are usually at a much lower resolution than interpretations of seismic velocity. Selby and Woodhouse (2002) carried out a global search for Q structure in the upper mantle based on surface waves, taking into account focussing and source effects. Their results show very small Q (strong attenuation) in a depth interval around 150 km in accordance with the global PREM model, where the LVZ between 90 and 220 km depth also exhibits strong attenuation with Q-values of around 60, which should be compared to values of more than 150 in the surrounding parts of the upper mantle (Fig. 9C). Der et al. (1986) find that the depth interval between 100 and 200 km below Eurasia displays particularly strong attenuation of seismic P- and S-waves compared to the surrounding depth intervals where the waves are hardly attenuated. Observations in the long-range seismic data set of the FENNOLORA experiment (Abramovitz et al., 2002) show that the Q-values in the LVZ are extremely small for S-waves compared to P-waves (c.f. Fig. 3). Morozov et al. (1998a) analyse the Q-values for P-waves in the upper mantle along the PNE profile QUARZ in Eurasia. They find that the LVZ below the 8° discontinuity is characterised by very strong attenuation with Q-values of 400 compared to 700–1400 for the surrounding depth intervals. This result also demonstrates that the attenuation in the LVZ is stronger for S- than P-waves.

4.4. The Lehmann discontinuity

In the previous section it was argued that the base of the LVZ may correspond to the upper mantle Lehmann discontinuity (Lehmann, 1961, 1964), and that this discontinuity is shallow (220 km deep or shallower) in cratonic regions and deep in tectonically active areas. This interpretation explains the finding by Gu et al. (2001) that the Lehmann discontinuity primarily is detected beneath parts of the continents with some depth variation, and not in the oceanic parts of the Earth. It is possible that the Lehmann discontinuity is deeper than the maximum search level in their investigation beneath other parts of the continents as well as beneath the oceans. Deuss and Woodhouse (2002) present the results of a global search for mantle reflectors based on SS precursors. They find that the largest number of robust reflections originates from a depth of around 220 km, mainly from continental but also oceanic areas. They attribute these reflectors to the Lehmann discontinuity. They also find evidence for reflections from deeper levels in other areas. Their results are displayed as maps of the occurrence of reflections from three depth levels of 220, 260, and 310 km, which show that the shallowest reflectors mainly are detected in cratonic areas of North America and Eurasia (Fig. 11A), that the deeper reflectors mainly are identified at the edge of the Siberian craton (Fig. 11B), and that the deepest reflectors are encountered mainly in tectonically active areas and the oceans, such as at eastern China and western North America (Fig. 11C). If we correlate these reflectors with the Lehmann discontinuity as the base of the LVZ, we find that the thickness of the LVZ depends systematically on the tectonic and thermal regime of the area under consideration, such that it is generally deep in active areas and shallow in stable areas.

4.5. Electrical conductivity

Only few studies of electrical conductivity have been carried out with high resolution at upper mantle depths due to the long periods required for obtaining the appropriate depth penetration. Early magnetotelluric results from more than 50 experiments indicate the presence of a general low-resistivity layer at a depth of 70–120 km in continental mantle which was correlated with the LVZ (Fournier et al., 1963). In a review of the results of electromagnetic studies of the northern Baltic Shield, Hjelt (1991) shows a series of depth soundings which include a steep decrease in resistivity in the depth interval below 90–130 km. Jones (1982) carried out a

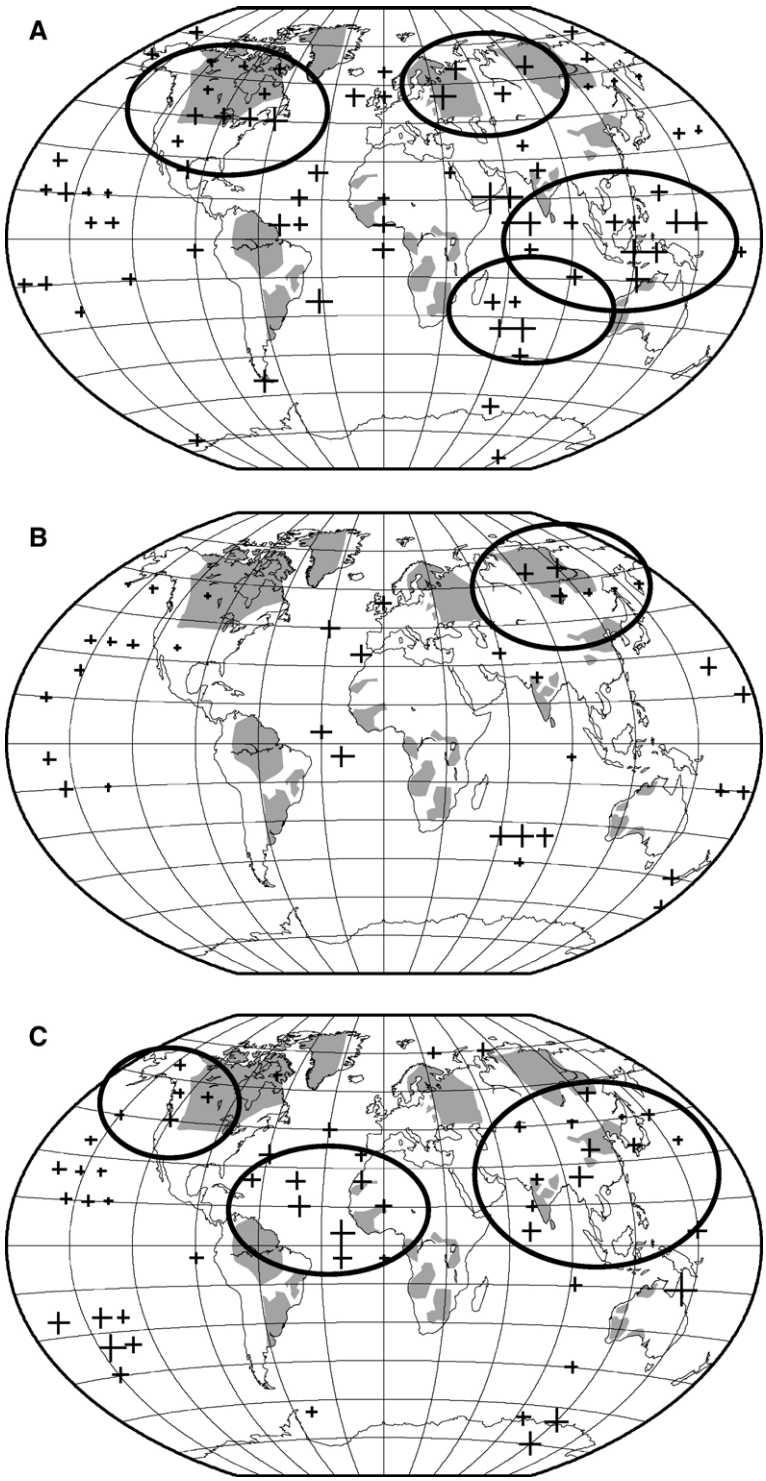

Fig. 11. Results of a global search for upper mantle discontinuities based on SS-precursors (after Deuss and Woodhouse, 2002) for three depth intervals: (A) 220, (B) 260, and (C) 310 km. Ellipses highlight the areas with high intensity of energy from discontinuities in the three intervals. The map also shows the location of the main Archaean and Palaeoproterozoic cratons. Notice how the shallow discontinuities are mainly identified at cratonic areas (A), and the deep discontinuities are detected at tectonically active areas at the edges of cratons (B, C).

Monte Carlo inversion of depth soundings in the northern Baltic Shield and found that all solutions require a sharp decrease in resistivity by more than one order of magnitude at depths between 105 and 180 km, depending on the location although, in retrospect, these interpretations may have been influenced by electrical noise from the atmosphere (Jones, 1999), such that the top of the high-conductivity zone can only be determined to depths between 100 and 200 km. The extensive electromagnetic project BEAR covers the whole of the Baltic Shield. The preliminary interpretation of the mantle conductivity structure shows gradually decreasing resistivity below a depth of 100 km. However, the resolution does, so far, not allow determination of the sharpness of this decrease, which may be between 0 and 200 km thick (Varentsov et al., 2002). ERCEUGT-Group (1992) discusses the results of a detailed depth sounding in Central Europe, again showing a sharp decrease in resistivity at 80–100 km depth. This result has been confirmed in a recent study of continental Europe by Simpson (2002). Jones (1999) presents a global summary table of the available deep electrical soundings, which shows that almost all deep electromagnetic interpretations identify a good conductor at a depth of 100–120 km or shallower, depending on location, except for three locations in northern Sweden, Senegal and central Australia where the layer of high conductivity is deeper than 120 km.

5. Reflectivity from the low velocity zone

The uppermost part of the mantle is strongly seismically reflective as documented by Hellfrich and Wood (2001), corresponding roughly to the lithospheric mantle. A strong, long-lasting coda is observed in all the available high-density record sections as a particular feature of the presence of the LVZ. The individual arrivals in this coda are randomly distributed at the scale lengths at which seismic waves from the upper mantle are observed, i.e. with a distance between observation points of the order of 15 km. The record section from the BABEL experiment (Fig. 4A) is an exceptional example. Although some smearing and leakage of energy may have been introduced by the stacking process, this section documents that none of the individual phases can be correlated over offset intervals longer than 10 km. This indicates that the maximum scale length of reflectors in the LVZ is of the order of 5 km, which is smaller than the size of the Fresnel zone at 100 km depth. Therefore, it is impossible to image individual reflectors in the zone with the available data. However, it is nevertheless possible to determine statistical parameters for the distribution of reflectors in the zone.

The individual reflectors probably require a 3-dimensional description, given the complexity of the observed signals. Modelling with the reflectivity method, i.e. calculation of synthetic seismograms in 3D for one-dimensional models, has shown that typical thicknesses of equivalent layers in the zone must be below 3–4 km (Perchuc and Thybo, 1996; Thybo and Perchuc, 1997; Nielsen et al., 2001). Tests of the scale lengths with finite difference calculations of synthetic seismograms are, so far, only possible with two-dimensional models. It would be preferable to calculate the synthetic seismograms for a scattering medium with a 3D distribution of the individual small scatterers (reflectors), but this is not possible with finite difference techniques implemented even on the largest super-computers currently available. Methods are currently being developed where mathematical transformations of the wave equation are used to make such calculations possible (cf. Margerin, 2006). It will be of interest to compare the results of calculations with these methods to the results from 2D calculations.

The 2D finite difference calculations are very computer demanding because the model has to be densely discretised, e.g. the model grid must include a node every 180 m in order to maintain numerical accuracy for mantle models at frequencies up to 10 Hz. The models extend to 2000 km offset and to depths of ca. 400 km. The synthetic seismograms are based on the viscoelastic wave equation, i.e. realistic models of attenuation are included and both P- and S-wave propagation is considered. Nielsen et al. (2002) and Nielsen et al. (2003) present examples of the effects of typical scale lengths in the LVZ on synthetic seismograms. Nielsen and Thybo (2006) present further documentation of the modelling and the possible influence of scattering from other depth intervals than the LVZ on the synthetic seismograms. Fig. 12 shows an example (c.f. Nielsen et al., 2002) of a statistical realisation of the scattering medium, which explains the observations of the scattering coda from cratonic areas (cf. the data examples in Figs. 3–8). The modelling shows that the medium in the LVZ (cf. Fig. 12) is characterized by typical scale lengths of 4–10 km, laterally, and 2–4 km, vertically, for a von Karman distribution of the parameters and a Hurst number of 0.5. Such media are thought to be close to fractal media (Holliger and Levander, 1992; Hurich and Smithson, 1997). The amplitude of the velocity contrasts is about 2–4%. Strong heterogeneity has also been demonstrated by use of the PNE data in a ca. 120 km wide zone around

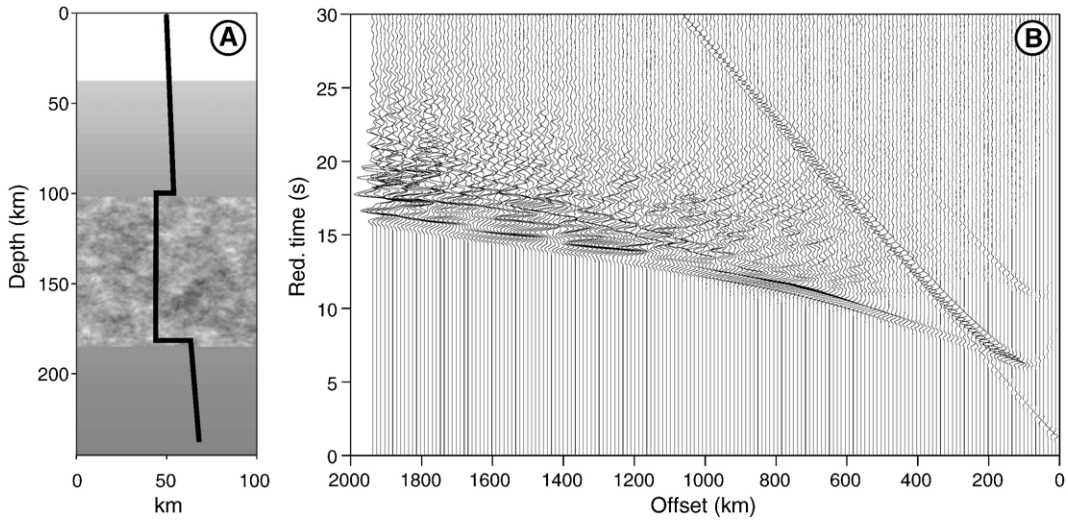

Fig. 12. Representation of the scattering medium in the upper mantle low velocity zone between 100 and 180 km depth with heterogeneity at a 5 by 3 km scale and an amplitude of 3% of the background velocity (A). Only 100 km is shown of the 2000 km long model. The curve shows the background velocity–depth profile. B) Corresponding synthetic seismic section, which reproduces the main features of the observed scattering from the LVZ (c.f. the data sections in Figs. 3–8).

the 410 km discontinuity with very similar properties, although at double scale length (Thybo et al., 2003b). One may notice that the qualitative appearance of the heterogeneity in the LVZ and the deeper upper mantle resembles a granitic rock except for the difference in scale length of a factor of 10,000. Systematic search has shown that other representations, such as elongated "gneiss-like" media, cannot explain the observed scattering. This result has implications for the discussion of scale invariance and fractal dimension of structure in the Earth.

A recent seismic study of the upper mantle below the Trans-Hudson Orogen in Canada has demonstrated strong reflectivity in the 80–160 km depth interval (Nemeth and Hajnal, 1998). The individual profiles are too short to allow determination of the velocity in this depth range, and the authors assume "normal" mantle velocity. They therefore interpret this reflectivity to be caused by shear zones in a ductile part of the mantle (Nemeth and Hajnal, 1998). However, the reflectivity is comparable to the reflectivity from the LVZ and occurs at the same offset interval and travel times.

This modelled scattering explains the observed reflectivity from the LVZ, typically observed between offsets of 500 and 1500 km with the longest coda observed at shortest offsets. The scattering is present at all observed frequencies. Another type of upper mantle scattering in a wave coda with an apparent velocity of 8 km/s has been proposed by, e.g. Tittgemeyer et al. (1996), and Ryberg and Wenzel (1999). These authors model this teleseismic Pn wave scattering by a high-frequency wave, which travels sub-horizontally in the upper mantle between the Moho and depths of ca. 120 km. They find that forward scattering in a sub-horizontal layering, given by a smooth Gaussian distribution with typical dimensions of 20 km, horizontally, and 1 km, vertically, can reproduce the observations at high frequencies (above 5 Hz). However, it has recently been shown that the considered teleseismic Pn phase also contains much lower frequencies than 5 Hz (Morozov et al., 1998b) which cannot be explained by this model (Nielsen and Thybo, 2004). The latter authors show that a whispering gallery phase, with multiple reflections from a scattering medium in the crust, may better explain all the observations and that all proposed distributions of scatterers in the interval above 100 km depth, will generate non-observed, strong low-frequency energy in the synthetic sections. Hence, there is no evidence for significant random scattering of seismic waves in the mantle above the LVZ. This depth interval also appears homogeneous at all seismic frequencies in normal incidence reflection seismic data, except for isolated individual reflectors, although long-range refraction seismic data indicates a sandwich-type of layering with intermixed high- and low-velocity layers in the uppermost mantle.

Receiver functions calculated from data from the Kaapvaal seismic experiment (Fig. 13) show details of seismic converters in the upper mantle (Gao et al., 2002). The image shows distinct converters from the Moho and the boundaries around the mantle transition zone. However, it also shows significant energy in the

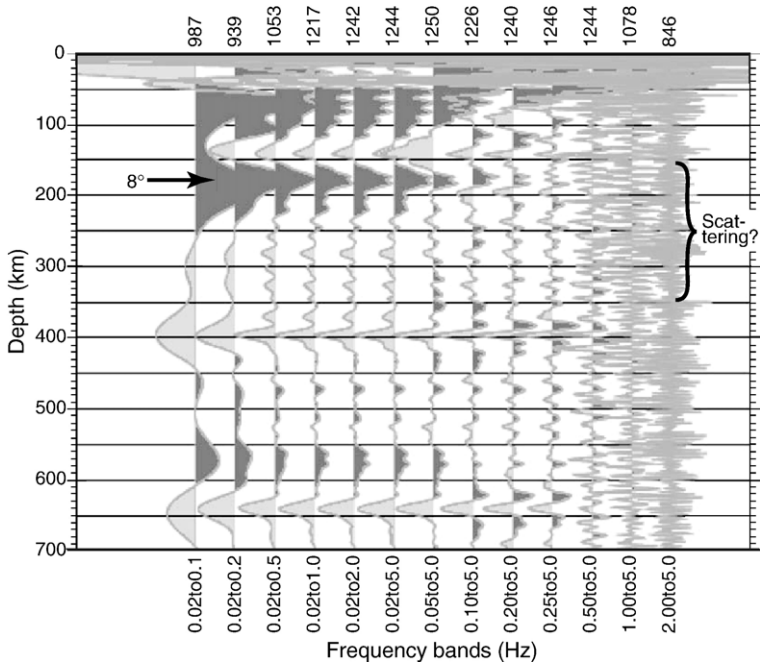

Fig. 13. Plot of seismic receiver functions calculated for data from S. Africa (after Gao et al., 2002), displayed with different frequency filters. The conversions from the transition zone are clearly imaged at around 400 and 650 km depth. Notice also the conversion from the expected depth (100 km) of the top of the low velocity zone (the 8° discontinuity) and the strong, later scattered energy, which may be caused by interference between waves from conversions from the scattering medium in the low velocity zone.

depth range between the Moho and the 410 km discontinuity, although with smaller amplitudes than the main upper mantle converters. Some of this energy may originate from crustal surface multiples. The section shows a distinct converter at around 120 km depth, which potentially may be related to the top of the LVZ (the 8° discontinuity). This conversion includes energy to the highest frequencies in the section, similar to the main converters, which indicates that this energy is not caused by crustal multiples. It is followed by a series of small amplitude energy down to 300 km depth, which is also observed at all frequencies. Gao et al. (2002) argue that, surprisingly, there are no distinct converters in the section between the conversions from the Moho and the 410 km discontinuity which may be related to the Lehmann discontinuity or traces of subducted slabs as often observed in other cratonic areas. They assume that heating by the African superplume may have destroyed features in the lithosphere in South Africa that may have been present earlier. However, the substantial energy between 100 and 300 km depth may show the effect of small scale scatterers, which are too small to be directly identified in the receiver function section but, nonetheless, are strong enough for identification, even after stacking. Because the individual scatterers in the LVZ are small, as modelled in other cratonic areas, the observed energy of the converted phases, probably, represents constructive interference between several small amplitude converted waves from individual converters.

6. Origin of the LVZ

The previous sections present observations of the global low velocity zone in the upper mantle in a depth interval below the 8° discontinuity at 100 km depth (±20 km). There is abundant evidence for the presence of this zone from application of a variety of seismic and other methods. In the stable continents, the zone has a slight velocity reduction and a low Q value, in particular for S-waves, compared to the surrounding intervals. The interval contains seismic scatterers on a scale of ca. 7×3 km (±2 km), although future 3D modeling may change the exact numbers. The base of the LVZ may correspond to the Lehmann discontinuity, which is shallow in cold, cratonic areas and deep in hot, active areas.

Many effects may contribute to the creation of seismic low velocity zones, seismic scattering effects, and the origin of the Lehmann discontinuity:

- Rocks close to the solidus or in a partially molten state

- The presence of fluids
- Change in anisotropy
- Change in rheology
- Metamorphic Phase Transformations
- Changes in composition
- Remnants of subducted slabs
- An irregular base of the lithosphere
- Magmatic intrusions

The depth to the upper mantle low velocity zone is almost the same (100 km) in all regions. This indicates that the existence of the zone should be explained in terms of metamorphic or other pressure dependent changes. None of the known significant phase transformations in peridotite corresponds to a pressure equivalent to 100 km depth.

Changes in composition of the mantle could potentially explain the presence of the LVZ. Large compositional changes are expected at subducted lithospheric slabs. If the slabs equilibrate at around the depth of interest (100–200 km), their presence could cause the LVZ, depending on the metamorphic state of the rocks. Tomographic inversion has provided images of subducting slabs from many locations around the world (e.g. Fukao and al., 2001). The images indicate that some subducting slabs continue into the deep mantle and that other slabs equilibrate at shallower depth, often at a depth of 800 km or perhaps as shallow as around the transition zone, but none of the images have provided evidence for buoyantly neutral slabs at depths levels above 300 km. Parts of the rocks in subducted slabs may melt to form silicate-rich melts, which are more dense than peridotitic rocks in the upper mantle. Such melts would be in neutral buoyancy just above the 410 km discontinuity and would therefore expectedly sink to about 410 km depth over geological time (Revenaugh and Meyer, 1997).

Compositional anomalies could also originate from variation in the degree of depletion due to magmatic activity and metasomatism. Artemieva (2003) suggests that the LVZ formed by metasomatic processes as the result of rifting processes in the East European Platform. She explains the enigmatic variation in topography and subsidence of shield and platform areas of the East European Platform by depth dependent chemical depletion in the upper mantle, through which a sharp metamorphic front may cause a low velocity zone in the lower part of the lithosphere (Artemieva, 2003). It is possible that such a metamorphic front may be situated at a depth of ca. 100 km in large parts of the East European Platform. However, the LVZ has been identified at the same depth in several places throughout Eurasia and on other continents, including both shield and platform areas. The large variation in topography and, therefore, depletion between these areas, suggest that there should be a strong variation in the depth to the LVZ, if generally caused by this mechanism. Hence, the suggested variation in composition may contribute to the existence of the LVZ in the East European Platform, but it is unlikely that this mechanism can explain its global occurrence. It is further unlikely that this model can explain the substantial heterogeneity observed in the LVZ which requires other mechanisms.

Anisotropy is a feature of the Earth's mantle, which is observed in many areas, and which is often ascribed to alignment of the rock minerals. Gung et al. (2003) interpret the Lehmann discontinuity under the continents as a change in anisotropic structure between frozen-in structure in the lithosphere and anisotropic structure from ongoing dynamic processes in the underlying asthenosphere. They suggest a similar origin of the oceanic G-discontinuity, despite its shallower level. Karato (1992) proposes that the Lehmann discontinuity results from a change in deformation mechanism. Dislocation creep in the shallow mantle results in an anisotropic structure above the Lehmann discontinuity, whereas diffusion creep causes an underlying isotropic mantle interval. This point of view is supported by seismological observations around Australia and the western Pacific (Gaherty and Jordan, 1995). There is undoubtedly large variation in anisotropy in the mantle, and it is very likely that the Lehmann discontinuity corresponds to a change in anisotropy. However, these models do not explain neither the observed systematic variation in depth to the Lehmann discontinuity nor the global occurrence of the LVZ at a relatively constant depth of 100 km. Instead they predict relatively constant depths to the Lehmann discontinuity, which is contrary to observations. The Russian PNE data was acquired along a series of profiles, including two perpendicular directions in eastern Siberia. Future interpretation of the velocity structure along these profiles may provide essential new information on possible anisotropy around the LVZ in the cratonic mantle.

The mechanisms discussed so far may explain some of the observations, or a regional occurrence of the LVZ, but not the global occurrence of the LVZ with its small variation in depth and large variation in thickness. Other mechanisms are therefore required with strong dependence on temperature and pressure. All the observations may be explained by the presence of inclusions of rocks with temperature close to the solidus (Thybo and

Perchuc, 1997). Small amounts of melt may lower the seismic velocity substantially. At solidus temperature, the velocity of the rocks may be 6% lower than at surface temperatures, and the existence of only trace amounts of melts may lower the velocity substantially as the slope of the velocity–temperature curve is very steep above the solidus (Sato et al., 1989a, Fig. 14). The decrease in velocity depends strongly on the melt geometry (Mavko, 1980). The velocity is substantially lowered at temperatures below and close to the solidus: e.g. the velocity decreases from a homologous temperature of T_m=0.8, to a value which may be 2–3% lowered at T_m=0.9 and 6% lowered at T_m=1.0 (T_m=T/$T_{solidus}$). A decrease of 2% is about the interpreted small velocity decrease at the top of the LVZ. It is likely that the temperature in the LVZ in cold cratonic regions is close to the solidus of mantle rocks in the presence of fluids. Sato et al. (1989b) show that rocks at a temperature close to the solidus exhibit strong attenuation of seismic waves, also in accordance with our observations. They further find that the top of such a zone will show a gradual change in seismic properties as indicated by the available data.

The LVZ is a global feature of the continental mantle. It is detected at a depth where the temperature (Artemieva and Mooney, 2001) is several hundreds of degrees lower than the solidus of dry peridotitic rocks. Normal temperatures in the upper mantle only exceed this dry solidus in a few isolated places, such as at mid-oceanic ridges and hot spots. In continental mantle dry melting may also take place around rift zones and at active magmatic centres, such as at continental flood basalt regions and at erupting kimberlite pipes. However, the situation is different if small amounts of fluids are present in the minerals (Fig. 14). The presence of water will lower the solidus substantially and increase the temperature interval between solidus and liquidus. Carbon dioxide in the mantle rocks will both lower the solidus and introduce a characteristic kink on the solidus curve (e.g. Wyllie, 1970, 1995). The kink follows the stability field of hornblende in the mantle rocks, such that the release of fluids from the hornblende component initiates the melting processes. The depth of melting is relatively constant for geotherms that cross the stability curve of the hornblende, i.e. in areas with high to moderate heat flow values. The exact depth to the kink depends on the chemistry of the rocks such that it is slightly shallower than 100 km for lherzolite and slightly deeper than 100 km for harzburgite, both in the presence of CO_2 and H_2O. In areas with very low heat flow, the geotherm may not reach the hornblende stability curve, and incipient melting may only be initiated at deeper levels. Sato et al. (1989a) notice that their results regarding the temperature effects on seismic

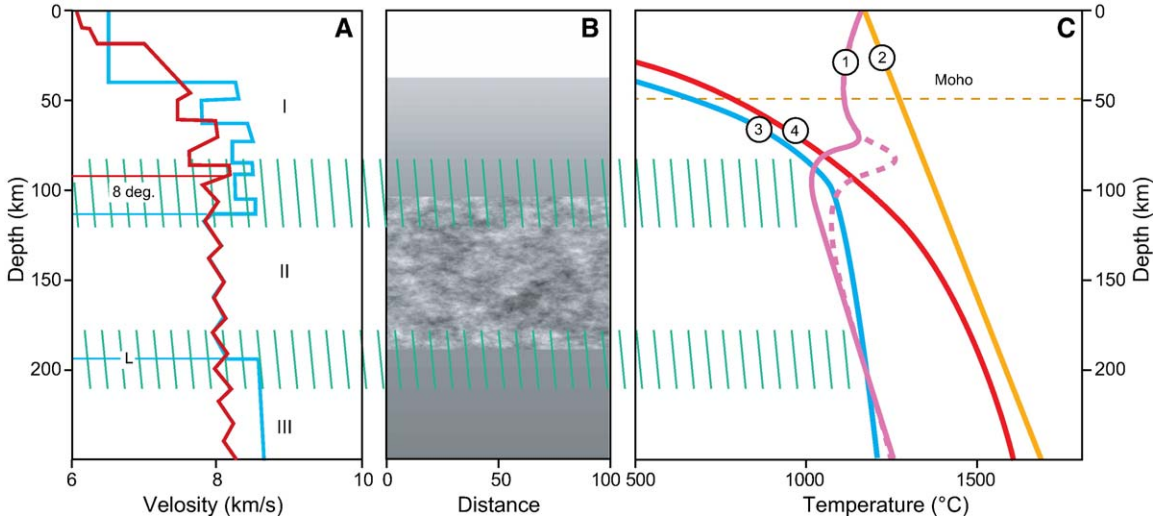

Fig. 14. A) Representative models of seismic velocity versus depth for cold (blue) and hot (red) areas. B) Representation of the 2D velocity variation in the LVZ that may explain the scattering of seismic waves. The amplitude variation is up to 3% of the background velocity, and the typical dimensions of the heterogeneity are 5 by 3 km. C) Solidus of peridotitic rocks; (1) including water and carbon dioxide and (2) dry together with typical geotherms: (3) for cold, stable cratonic areas, and (4) for hot, tectonically active areas. Notice how the geotherms cross the wet solidus at approximately the same depth due to the kink on the solidus. The hot geotherm extends above the solidus to large depth whereas the cold geotherm crosses the solidus at a shallow depth of around 200 km. Notice that this model also predicts the existence of the LVZ even if the cold geotherm does not cross the solidus, but instead only reaches temperatures within 20% of the solidus because the seismic velocity decreases substantially (by 6%) in the temperature interval from 80% of the solidus to the solidus.

velocity close to the solidus for dry peridotitic rocks are also valid for wet rocks. We may conclude that the temperature effect on wet mantle rocks will lower the seismic velocity for homologous temperatures higher than 0.8. Such temperatures are expected almost everywhere in continental mantle below depths of 100–150 km, even in areas with very low heat flow (Artemieva and Mooney, 2001).

The pressure at the kink of the solidus is equivalent to a depth of 70–110 km, which is close to the characteristic depth to the LVZ. The combined presence of even small amounts of water and carbon dioxide in the upper mantle lowers the melting temperatures of the rocks below depths of 70–110 km, in particular just beneath the characteristic kink on the solidus. The exact location of the solidus depends on the amounts of fluids being present and on the proportion between water and carbon dioxide (Wyllie, 1995). The latter proportion may change the solidus temperature by some hundreds of degrees. Only trace amounts of volatiles (of the order of 100 ppm or less) are required to initiate the metamorphic processes if only the temperature is sufficiently high (Wyllie et al., 1990). At temperatures between the solidus and the liquidus, the amount of melt depends primarily on the amount of available fluids. The amount of fluids in the mantle is subject to discussion, and there is undoubtedly substantial regional variation. Fluids are consumed in those zones where incipient melting takes place or where the minerals can store the fluids, such that the fluids will flow into these zones. This migration may create pockets or zones with low seismic velocities and strong attenuation due to the high percentages of fluids or partial melt in otherwise dryer, solid rocks, in accordance with the observation of strong seismic scattering in the LVZ by bodies at typical scale lengths of 7×3 km.

Partial melting of the mantle rocks depends heavily on the actual mantle temperatures. There is little doubt that the mantle temperatures (Pollack and Chapman, 1977) are substantially higher than the wet solidus below a depth of 80–120 km in most continental areas (c.f. Fig. 14). In these areas, the amount and configuration of melt primarily depend on the amount and type of fluids that have been available for the melting process. The melt remains below the depth level of 80–100 km, which indicates that the amount of melt is small due to limited availability of fluids. Buoyant ascent of magma would be expected if large amounts of melt were formed. Hence, the melting process is probably primarily controlled by the available amount of fluids.

Temperatures at depths of around 100 km in the cratonic mantle are estimated from heat flow measurements to be at least 800–900 °C or higher everywhere except for in mid-eastern Siberia, western Africa and the eastern Baltic Shield, where temperatures as low as 600 °C have been estimated (Artemieva and Mooney, 2001). These temperatures of 800–900 °C are close to the solidus (Fig. 14). We conclude that the temperatures in normal cratonic mantle are within 10% of the solidus temperature at depths below 100 km. This predicts substantial reduction in seismic velocities (by >2–3%) and Q-values. Heterogeneity of the mantle rocks and the actual distribution of the limited amount of fluids will tend to create bodies or inclusions of rocks with reduced velocity and Q-value in an otherwise unaffected matrix of rocks. It cannot be excluded that the temperatures locally may exceed the solidus such that incipient melting may take place, depending on the exact temperature, the amount of fluids present, and the relative proportion of water and carbon dioxide. The effects on seismic waves will qualitatively be the same, whether or not the depth interval contains partially molten rocks. The particularly strong attenuation of S-waves, observed in the Baltic Shield, indicates the presence of melts in the LVZ. In the cratonic areas with the lowest heat flow, the estimated temperatures at 150 km depth are around 800–900° (Artemieva and Mooney, 2001). This indicates temperatures within 10% of the solidus (Fig. 14) in the depth interval of 120–160 km, corresponding to a reduction of 3% in P-wave velocity (Sato et al., 1989a,b Fig. 14). Even if the total amount of available fluid is small and the fluids are concentrated in pockets, this reduction in velocity is sufficient to explain the observed velocity reduction in the coldest cratonic areas. The melting process is mainly controlled by the interaction between volatiles and the hornblende component of the mantle rocks. We may expect that the melts will be concentrated in those zones where melting was first initiated and that their distribution will depend on pre-existing chemical heterogeneity. The resulting clustering of the melt will contribute to the overall heterogeneity of the zone at seismic wavelengths.

The presence of free fluids in mantle rocks may also reduce the seismic velocity (Mavko, 1980). If the fluids accumulate in localized patches, their presence may lead to substantial scattering of seismic waves that propagate through the zone of interest at seismic frequencies. Karato and Jung (1998) argue that the presence of fluids will lower the seismic velocity through anelastic relaxation much more than the presence of partial melt. This implies that melting may increase the seismic

velocity compared to a wet rock lithology by the removal of water. On the other hand, Sato et al. (1989b) argue that temperatures close to the solidus will lead to decreased seismic velocities and *Q*-values, independent of the presence of fluids. In any case, it is difficult to reconcile how free fluid accumulations in the available pore volume may be constrained to a depth interval below a fixed level of 100 km. There is no viable explanation that free fluids should be constrained to a certain depth interval. Instead, depending on the available amount, free fluids will dissolve in the crystals of the mantle rocks and affect the metamorphic processes. Laboratory experiments have shown that the presence of volatile components, depending on their composition, will bring the rocks to a state close to the solidus temperature for the predicted geotherms of both cold and hot areas (Wyllie, 1970, 1995; Fig. 14). As such, it is unlikely that there are free fluids present below 100 km depth, because the fluids will react with the mantle minerals and, depending on the actual temperature, form partial melt.

High-frequency, normal-incidence reflection seismic images of the upper mantle often show sub-horizontal reflections at 20–24 s twt. Such reflections are observed in a variety of tectonic and cratonic areas. Several explanations for their origin have been suggested, including magmatic intrusions, the base of the lithosphere, mantle shear zones, and rheologic layering (Steer et al., 1998). The results from the MONA LISA project in the North Sea (Fig. 15) show a strong mantle reflection at about the same travel time of 22 s twt on two profiles at their common crossing point (MONA LISA Working Group, 1997). The presence of this reflection on both profiles demonstrates that it cannot be caused by sideswipe reflections or other artefacts and that the reflection point must be located beneath the cross point between the two profiles. The depth to the reflector is approximately 80 km, which is just above the LVZ in this area. It is therefore tempting to relate the occurrence of such reflections to the LVZ. The reflectors are too shallow to correspond to the base of the lithosphere. Considering that water is important for the development of the LVZ, a rheological cause of the reflectors is also unlikely. Hence, magmatic intrusions or sills in the mantle are the most probable explanation. A likely mechanism of formation relates to temporal buoyancy instabilities, which may cause the melt to

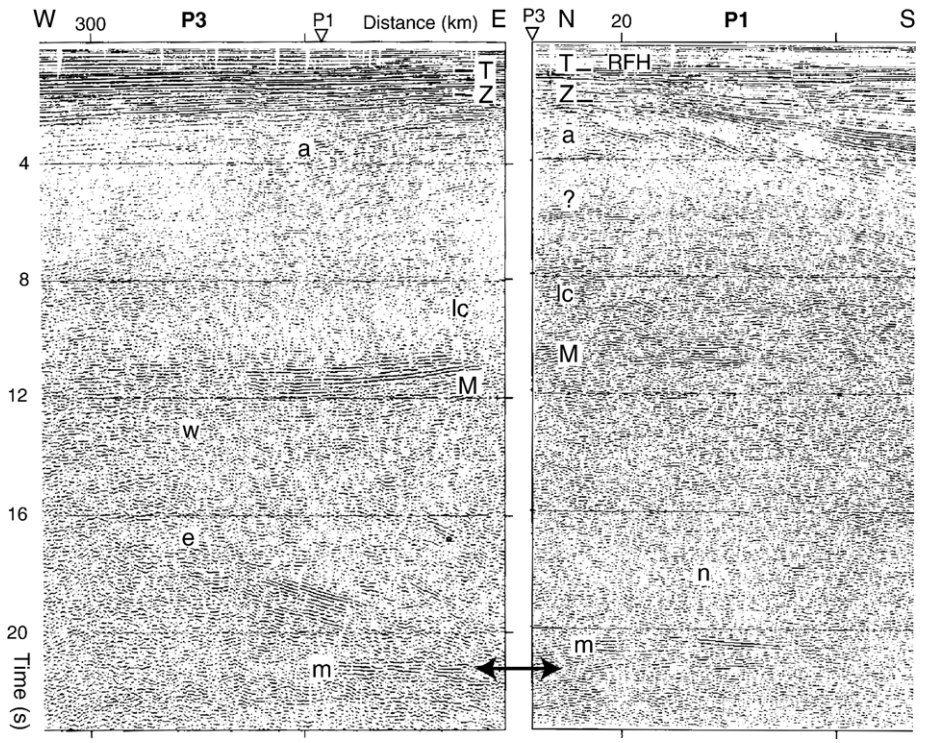

Fig. 15. Parts of two crossing, normal incidence reflection seismic profiles from the North Sea area (after MONA LISA Working Group, 1997). The reflection from the base of the crust arrives at around 11 s twt (*M*). The pronounced reflections at 21–23 s twt (*m*) are from the upper mantle, at a depth of approximately 80 km. The two profiles are perpendicular which demonstrates that the sub-horizontally reflections recorded on both profiles can only originate from below the cross point between the two profiles. These reflections may image sill like bodies in the uppermost mantle that may have formed from ascending magma from the LVZ, which is only 20 km deeper than these reflectors.

migrate upwards from the LVZ. Due to the pressure-inversion of the solidus at the kink, such melts will solidify immediately after their escape from the LVZ, depending on the speed of ascent. These trapped magmatic rocks may have strong contrast in acoustic impedance to the host rock, which will explain their high reflection coefficients.

7. Conclusions

The available high-resolution, explosion seismic data indicates the global existence of the uppermost mantle low velocity zone (LVZ) below a depth of approximately 100 km, i.e. beneath the 8° discontinuity. This finding is supported by other seismological evidence: (1) velocity structure based on inversion of regional and global surface wave data, also indicative of substantial S-wave anisotropy in the zone, (2) primary and multiple reflections of body waves from the bounding interfaces: the 8° discontinuity and the Lehmann discontinuity, (3) receiver functions detect a seismic converter at ca. 100 km as well as indicate scattered conversions in the interval below 100 km depth, and (4) small Q-values in the zone as based on body and surface wave studies. Currently available methods for tomographic inversion of teleseismic waves cannot detect a low velocity zone because the inversion is based on relative arrival times. However, models of absolute velocity based on regional inversion of travel time data from controlled surface sources include the mantle low velocity zone. Long-period electromagnetic studies indicate the existence of material with high conductivity in the upper mantle, in most areas beneath a depth of 80–120 km, but deeper in some other areas. Data from the extensive magnetotelluric BEAR project have indicated substantial uncertainty on the estimated depths to the good conductors in the upper mantle. As such we may conclude that the upper mantle low velocity zone exists in large parts of the continental mantle in an interval beneath ca. 100 km depth. This indicates that the zone is a global feature.

The characteristics of the low velocity zone may be summarized as:

- 1–5% lower velocity than in the surrounding intervals,
- strong attenuation of seismic waves, in particular S-waves,
- low seismic resistivity,
- it is a global continental feature,
- it is located in a depth interval below 100 ±20 km,
- it includes seismic scatterers on a typical scale length of ca. 7×3 km (±2 km),
- its base is a seismic refractor at variable depth (the Lehmann discontinuity), which is shallow (150–250 km deep) in cold, stable areas and deep (250–400 km deep) in hot, active areas.

Because of the relatively constant depth and the systematic variation in thickness, it is most probable that the temperatures of the rocks in the LVZ are close to the solidus, and in some the areas the rocks may even be in a partially molten state. A characteristic kink on the solidus curve for peridotitic rocks in the presence of water and carbon dioxide may explain the almost constant depth to the LVZ. Even small amounts of fluids (<100 ppm) are sufficient for a substantial reduction of the solidus temperature and widening of the area between the solidus and liquidus. Where present, melts formed by this mechanism are kept in an unstable equilibrium: They are prone to solidify if they migrate upwards above the kink at ca. 100 km depth because their temperature is below solidus at shallow depth. The systematic variation in thickness of the LVZ indicates that the Lehmann discontinuity marks the transition from rocks, which are close to solidus or partially molten, to fully solid rocks. The LVZ is thin in cold stable cratons and thick in hot, active regions. The importance of this anomalous zone of the upper mantle for the rheology is not yet clear. Nevertheless, we expect that it may have strong influence on the mechanisms of plate motion.

Acknowledgments

Discussions with T. Abramovitz, A. Berthelsen, L. Nielsen (Copenhagen), and E. Perchuc (Warsaw) are appreciated. A. Shulgin (Moscow, Berkeley) calculated Fig. 10C and L. Nielsen (Copenhagen) calculated Fig. 12. A. Levander (Houston) provided a very thoughtful review and kindly provided the seismic section in Fig. 7. This research received financial support from the Carlsberg Foundation and the Danish Natural Science Research Council.

References

Abramovitz, T., Thybo, H., Perchuc, E., 2002. Tomographic inversion of seismic P- and S-wave velocities from the Baltic Shield based on FENNOLORA data. Tectonophysics 358, 151–174.

Anderson, D.L., 1989. Theory of the Earth. Blackwell, Oxford. 366 pp.

Ansorge, J., Mueller, S., 1973. The P-wave structure of the Uppermost Mantle in Europe based on long-range explosion observations. Zeitschrift fuer Geophysik 39 (3), 385–394.

Artemieva, I.M., 2003. Lithospheric structure, composition, and thermal regime of the East European Craton: implications for the

subsidence of the Russian platform. Earth and Planetary Science Letters 213, 431–446.
Artemieva, I.M., Mooney, W.D., 2001. Thermal thickness and evolution of Precambrian lithosphere: a global study. Journal of Geophysical Research 106 (B8), 16387–16414.
BABEL Working Group, 1991. Recording marine airgun shots at offsets between 300 and 700 km. Geophysical Research Letters 18 (4), 645–648.
Bijwaard, H., Spakman, W., Engdahl, E.R., 1998. Closing the gap between regional and global travel time tomography. Journal of Geophysical Research B, Solid Earth and Planets 103 (12), 30055–30078.
Bondar, I., Ryaboy, V., 1997. Regional Travel-Time Tables for the Baltic Shield Region. Center for Monitoring Research, Arlington.
Boschi, L., Ekström, G., 2002. New images of the Earth's upper mantle from measurements of surface wave phase velocity anomalies. Journal of Geophysical Research 107 (B4). doi:10.1029/2000JB000059.
Bowman, J.R., Kennett, B.L.N., 1990. An investigation of the upper mantle beneath NW Australia using a hybrid seismograph array. Geophysical Journal International 101 (2), 411–424.
Burdick, L.J., 1978. The upper mantle P velocity structure of the western United States. Journal of Geophysical Research 83 (B4).
Calcagnile, G., 1991. Deep structure of Fennoscandia from fundamental and higher mode dispersion of Rayleigh waves. Tectonophysics 195, 139–149.
Darbyshire, F.A., 2003. Crustal structure across the Canadian High Arctic region from teleseismic receiver function analysis. Geophysical Journal International 152, 372–391.
Darbyshire, F.A., 2005. Upper mantle structure of Arctic Canada from Rayleigh wave dispersion. Tectonophysics 405, 1–23.
Der, Z.A., Lees, A.C., Cormier, V.F., 1986. Frequency dependence of Q in the mantle underlying the shield areas of Eurasia: Part III. The Q model. Geophysical Journal of the Royal Astronomical Society 87 (3), 1103–1112.
Deuss, A., Woodhouse, J.J., 2002. A systematic search for mantle discontinuities using SS-precursors. Geophysical Research Letters 29 (8), 1249. doi:10.1029/2002GL014768.
Dziewonski, A.M., Anderson, D.L., 1981. Preliminary reference Earth model. Physics of the Earth and Planetary Interiors 25 (4), 297–356.
ERCEUGT-Group, 1992. An electrical resistivity crustal section from the Alps to the Baltic Sea (central segment of the EGT). Tectonophysics 207, 123–139.
Fournier, H.G., Ward, S.H., Morrison, H.F., 1963. Magnetotelluric Evidence for the Low Velocity Layer. University of California, Berkeley.
Fuchs, K., 1997. Upper mantle heterogeneities from active and passive seismology. NATO Science Series. Partnership Sub-series 1, Disarmament Technologies, vol. 17. Kluwer Academic Publishers, Dordrecht, Netherlands. 366 pp.
Fukao, Y., et al.,, 2001. Stagnant slabs in the upper and lower mantle transition region. Reviews of Geophysics 39 (3), 291–323.
Gaherty, J.B., Jordan, T.H., 1995. Lehmann discontinuity as the base of an anisotropic layer beneath continents. Science 268 (5216), 1468–1471.
Gao, S.S., Silver, P.G., Liu, K.H., Group, K.S., 2002. Mantle discontinuities beneath southern Africa. Geophysical Research Letters 29 (10). doi:10.1029/2001GL013834.
Given, J.W., Helmberger, D.V., 1980. Upper mantle structure of northwestern Eurasia. JGR. Journal of Geophysical Research B 85 (12), 7183–7194.
Gorman, A.R., et al., 2002. Deep Probe; imaging the roots of western North America. Canadian Journal of Earth Sciences 39, 375–398.
Grand, S.P., Helmberger, D.V., 1984. Upper mantle shear structure of North America. Geophysical Journal of the Royal Astronomical Society 76 (2), 399–438.
Green, R.W.E., Hales, A.L., 1968. The travel times of P waves to 30 degrees in the central United States and upper mantle structure. Bulletin of the Seismological Society of America 58 (1), 267–289.
Gu, Y.J., Dziewonski, A.M., Ekström, G., 2001. Preferential detection of the Lehmann discontinuity beneath continents. Geophysical Research Letters 28, 4655–4658.
Guggisberg, B., Berthelsen, A., 1987. A two-dimensional velocity model for the lithosphere beneath the Baltic Shield and its possible tectonic significance. Terra Cognita 7, 631–638.
Guggisberg, B., Kaminski, W., Prodehl, C., 1991. Crustal structure of the Fennoscandian Shield; a travel time interpretation of the long-range FENNOLORA seismic refraction profile. Tectonophysics 195, 105–137.
Gung, Y., Panning, M., Romanowicz, B., 2003. Global anisotropy and the thickness of continents. Nature 422, 707–711.
Hales, A.L., 1991. Upper mantle models and the thickness of the continental lithosphere. Geophysical Journal International 105 (2), 355–363.
Hauser, F., Prodehl, C., Schimmel, M., 1990. A Compilation of Data from the FENNOLORA Seismic Refraction Experiment 1979, Geophysical Institute, Univ. Karlsruhe.
Hellfrich, G.R., Wood, B.J., 2001. The Earth's mantle. Nature 412, 501–507.
Helmberger, D.V., 1973. On the structure of the low velocity zone. The Geophysical Journal of the Royal Astronomical Society 34 (2), 251–263.
Helmberger, D.V., Engen, G.R., 1974. Upper mantle shear structure. Journal of Geophysical Research 79 (26), 4017–4028.
Henstock, T.J., Levander, A., Deep Probe Working Group, 1998. Probing the Archean and Proterozoic lithosphere of western North America. GSA Today 8 (1–5), 16–17.
Hill, D.P., 1972. Crustal and upper mantle structure of the Columbia Plateau from long range seismic-refraction experiments. Geological Society of America Bulletin 83, 1639–1648.
Hill, D.P., 1974. Phase shift and pulse distortion in body waves due to internal caustics. Bulletin of the Seismological Society of America 64 (6), 1733–1742.
Hill, R.N., Levander, A.R., 1984. Resonance of low-velocity layers with lateral variations. Bulletin of the Seismological Society of America 74, 521–537.
Hirn, A., Steinmetz, L., Kind, R., Fuchs, K., 1973. Long range profiles in western Europe; II, fine structure of the lower lithosphere in France (southern Bretagne). Zeitschrift fuer Geophysik 39 (3), 363–384.
Hjelt, S.-E., 1991. Geoelectric studies and conductivity structures of the eastern and northern parts of the Baltic Shield. Tectonophysics 189, 249–260.
Holliger, K., Levander, A.R., 1992. A stochastic view of lower crustal fabric based on evidence from the Ivrea Zone. Geophysical Research Letters 19 (11), 1153–1156.
Hurich, C.A., Smithson, S.B., 1997. Compositional variation and the origin of deep crustal reflections. Earth and Planetary Science Letters 85 (4), 416–426.
Iyer, H.M., Pakiser, L.C., Stuart, D.J., Warren, D.H., 1969. Project early rise: seismic probing of the upper mantle. Journal of Geophysical Research 74, 4409–4439.

Jeffreys, H., 1936. The structure of the earth down to the 20E discontinuity. Monthly Notices of the Royal Astronomical Society, Geophysical Supplement 3 (9), 401–422.

Jones, A.G., 1982. Observations of the electrical asthenosphere beneath Scandinavia. The structure of the lithosphere–asthenosphere in Europe and the North Atlantic. Tectonophysics 90 (1–2), 37–55.

Jones, A.G., 1999. Imaging the continental upper mantle using electromagnetic methods. Lithos 48, 57–80.

Karato, S.-I., 1992. On the Lehmann discontinuity. Geophysical Research Letters 19 (22), 2255–2258.

Karato, S., Jung, H., 1998. Water, partial melting and the origin of the seismic low velocity and high attenuation zone. Earth and Planetary Science Letters 157, 193–207.

Kennett, B.L.N., Engdahl, E.R., 1991. Travel times for global earthquake location and phase identification. Geophysical Journal International 105 (2), 429–465.

Knopoff, L., 1972. Observation and inversion of surface-wave dispersion. Tectonophysics 13, 497–519.

Kumar, P., Kind, R., Hanka, W., Wylegalla, K., Reigber, Ch., Yuan, X., Woelbern, I., Schwintzer, P., Fleming, K., Dahl-Jensen, T., Larsen, T.B., Schweitzer, J., Priestley, K., Gudmundsson, O., Wolf, D., 2005. The lithosphere–asthenosphere boundary in the North West Atlantic Region. Earth and Planetary Science Letters 226, 249–257.

Lehmann, I., 1936. Publications du Bureau Central Seismologique International. Serie A, Travaux Scientifiques 14, 3.

Lehmann, I., 1961. S and the structure of the upper mantle. Geophysical Journal, London 4, 124–138.

Lehmann, I., 1964. On the velocity of P in the upper mantle. Bulletin of the Seismological Society of America 54, 1097–1103.

Margerin, L. Attenuation, transport and diffusion of scalar waves in textured random media. Tectonophysics 416, 229–244. doi:10.1016/j.tecto.2005.11.015 (this volume).

Masse, R.P., 1973. Shear velocity distribution beneath the Canadian Shield. Journal of Geophysical Research 78 (29), 6943–6950.

Masse, R.P., Landisman, M., Jenkins, J.B., 1972. An investigation of the Upper Mantle compressional velocity distribution beneath the Basin and Range Province. The Geophysical Journal of the Royal Astronomical Society 30 (1), 19–36.

Mavko, G.M., 1980. Velocity and attenuation in partially molten rocks. In: Kovach Robert, L., Nur Amos, M. (Eds.), Stanford Q Conference. Journal of Geophysical Research B. American Geophysical Union, Washington, DC, United States, pp. 5173–5189.

Mayer, R.O., Mueller, S., 1973. The gross velocity–depth distribution of P- and S-waves in the upper mantle of Europe from earthquake observations. Zeitschrift fuer Geophysik 39 (3), 395–410.

Mechie, J., et al., 1993. P-wave mantle velocity structure beneath northern Eurasia from long-range recordings along the profile Quartz. Physics of the Earth and Planetary Interior 79 (1–2), 269–286.

Miller, K.C., et al., 1997. Crustal structure along the west flank of the Cascades, western Washington. Journal of Geophysical Research B, Solid Earth and Planets 102 (8), 17857–17873.

Mohorovicic, A., 1909. Das beben vom 8.X.1909. Ahrbuch Met. Obs. Zagreb, vol. 9, pp. 1–63.

MONA LISA Working Group, 1997. MONA LISA; deep seismic investigations of the lithosphere in the southeastern North Sea. Tectonophysics 269 (1–2), 1–19.

Montelli, R., et al., 2004. Finite-frequency tomography reveals a variety of plumes in the mantle. Science 303, 338–343.

Morozov, I.B., Morozova, E.A., Smithson, S.B., Solodilov, L.N., 1998a. 2D image of seismic attenuation beneath the deep seismic sounding profile QUARTZ. Pure and Applied Geophysics 153, 311–343.

Morozov, I.B., Morozova, E.A., Smithson, S.B., Solodilov, L.N., 1998b. On the nature of the teleseismic Pn phase observed on the ultralong-range profile "Quartz" Russia. Bulletin of the Seismological Society of America 88 (1), 62–73.

Morozova, E.A., Morozov, I.B., Smithson, S.B., Solodilov, L., 2000. Lithospheric boundaries and upper mantle heterogeneity beneath Russian Eurasia; evidence from the DSS profile QUARTZ. Tectonophysics 329, 333–344.

Nemeth, B., Hajnal, Z., 1998. Structure of the lithospheric mantle beneath the Trans-Hudson Orogen, Canada. Tectonophysics 288, 93–104.

Niazi, M., Anderson, D.L., 1965. Upper mantle structure of western North America from apparent velocities of P waves. Journal of Geophysical Research 70, 4633–4640.

Nielsen, L., Thybo, H., 2003. The origin of teleseismic Pn waves: multiple crustal scattering of upper mantle whispering gallery phases. Journal of Geophysical Research 108 (B10), 2460. doi:10.1029/2003JB002487.

Nielsen, L., Thybo, H., 2004. Location of the Carlsberg Fault zone from seismic controlled-source fan recordings. Geophysical Research Letters 31, L07621. doi:10.1029/2004GL019603.

Nielsen, L., Thybo, H., 2006. Identification of crustal and upper mantle heterogeneity by modelling of controlled-source seismic data. Tectonophysics 416, 209–228. doi:10.1016/j.tecto.2005.11.020 (this volume).

Nielsen, L., Thybo, H., Solodilov, L., 1999. Seismic tomographic inversion of Russian PNE data along profile Kraton. Geophysical Research Letters 26 (22), 3413–3416.

Nielsen, L., Thybo, H., Egorkin, A.V., 2001. Constraints on reflective bodies below the 8 degrees discontinuity from reflectivity modelling. Geophysical Journal International 145 (3), 759–770.

Nielsen, L., Thybo, H., Egorkin, A.V., 2002. Implications of seismic scattering below the 8 degrees discontinuity along PNE profile Kraton. Tectonophysics 358, 135–150.

Nielsen, L., Thybo, H., Levander, A., Solodilov, L., 2003. Origin of upper mantle seismic scattering evidence from Russian PNE data. Geophysical Journal International 154, 196–204.

Panza, G.F., 1981. The resolving power of seismic surface waves with respect to crust and upper mantle structural models. In: Cassinis, R. (Ed.), The Solution of the Inverse Problem in Geophysical Interpretation. Plenum Publ. Corp, pp. 39–77.

Pavlenkova, G.A.P.K., Cipar, J., 2002. 2D model of the crust and uppermost mantle along RIFT profile, Siberian craton. Tectonophysics 355, 171–186.

Perchuc, E., Thybo, H., 1996. A new model of upper mantle P-wave velocity below the Baltic Shield; indication of partial melt in the 95 to 160 km depth range. Tectonophysics 253 (3–4), 227–245.

Pollack, H.N., Chapman, D.S., 1977. On the regional variation of heat flow, geotherms, and lithospheric thickness. Tectonophysics 38 (3–4), 279–296.

Pontevivo, A., Thybo, H., 2006. Test of the upper mantle low velocity layer in Siberia with surface waves. Tectonophysics 416, 113–131. doi:10.1016/j.tecto.2005.11.015 (this volume).

Priestley, K., Debayle, E., 2003. Seismic evidence for a moderately thick lithosphere beneath the Siberian Platform. Geophysical Research Letters 30 (3), 1118–1121.

Priestley, K.F., Cipar, J., Egorkin, A., Pavlenkova, N.I., 1994. Upper-mantle velocity structure beneath the Siberian Platform. Geophysical Journal International 118 (2), 369–378.

Revenaugh, J., Meyer, R., 1997. Seismic evidence partial melt within a possibly ubiquitous low-velocity layer at the base of the mantle. Science 277 (5326), 670–673.

Romanowicz, B., Gung, Y., 2002. Superplumes from the core-mantle boundary to the lithosphere: implications for heat flux. Science 296, 513–516.

Romney, C., et al., 1962. Travel times and amplitudes of principal body phases recorded from Gnome. Bulletin of the Seismological Society of America 52, 1057–1074.

Ryberg, T., Wenzel, F., 1999. High-frequency wave propagation in the uppermost mantle. Journal of Geophysical Research B, Solid Earth and Planets 104 (5), 10655–10666.

Ryberg, T., Wenzel, F., Mechie, J., Egorkin, A., Fuchs, K., Soloddilov, L., 1996. Two-dimensional velocity structure beneath northern Eurasia derived from the super long-range seismic profile Quartz. Bulletin of the Seismological Society of America 86 (3), 857–867.

Sato, H., Sacks, I.S., Murase, T., 1989a. The use of laboratory velocity data for estimating temperature and partial melt fraction in the low-velocity zone; comparison with heat flow and electrical conductivity studies. Journal of Geophysical Research, B, Solid Earth and Planets 94 (5), 5689–5704.

Sato, H., Sacks, I.S., Murase, T., Muncill, G.E., Fukuyama, H., 1989b. Qp-melting temperature relation in peridotite at high pressure and temperature; attenuation mechanism and implications for the mechanical properties of the upper mantle. Journal of Geophysical Research B, Solid Earth and Planets 94 (8), 10,647–10,661.

Selby, N.D., Woodhouse, J.H., 2002. The Q structure of the upper mantle: constraints from Rayleigh wave amplitudes. Journal of Geophysical Research 107 (B5). doi:10.1029/2001JB000257.

Simpson, F., 2002. A comparison of electromagnetic distortion and resolution of upper mantle conductivities beneath continental Europe and the Mediterranean using islands as windows. Physics of the Earth and Planetary Interiors 129, 117–130.

Spakman, W., van der Lee, S., van der Hilst, R., 1993. Travel-time tomography of the European–Mediterranean mantle down to 1400 km. Physics of Earth and Planetary Interiors 79, 3–74.

Stangl, R., 1990. Die Struktur der Lithosphäre in Schweden, abgeleitet aus einer gemeinsamen Interpretation der P- und S-Wellen Registrierungen auf dem FENNOLORA-Profil, University of Karlsruhe. 187 pp.

Steer, D.N., Knapp, J.H., Brown, L.D., 1998. Super-deep reflection profiling; exploring the continental mantle lid. Deep Seismic Profiling of the Continents; I, General Results and New Methods, vol. 286(1–4), pp. 111–121.

Suhadolc, P., Panza, G.F., Mueller, S., 1990. Physical properties of the lithosphere–asthenosphere system in Europe. Tectonophysics 176 (1–2), 123–135.

Sultanov, D.D., Murphy, J.R., Rubinstein, K.D., 1999. A seismic source summary for Soviet peaceful nuclear explosions. Bulletin of the Seismological Society of America 89 (3), 640–647.

Thybo, H., Perchuc, E., 1997. The seismic 8 degrees discontinuity and partial melting in continental mantle. Science 275 (5306), 1626–1629.

Thybo, H., Zhou, S., Perchuc, E., 2000. Intraplate earthquakes and a seismically defined lateral transition in the upper mantle. Geophysical Research Letters 27, 3953–3956.

Thybo, H., Ross, A.R., Egorkin, A.V., 2003a. Explosion seismic reflections from the earth's core. Earth and Planetary Science Letters 216, 693–702.

Thybo, H., Nielsen, L., Perchuc, E., 2003b. Seismic scattering at the top of the mantle transition zone. Earth and Planetary Science Letters 216, 259–269.

Tittgemeyer, M., Wenzel, F., Fuchs, K., Ryberg, T., 1996. Wave propagation in a multiple-scattering upper mantle; observations and modelling. Geophysical Journal International 127 (2), 492–502.

van der Lee, S., Nolet, G., 1997. Upper mantle S velocity structure of North America. Journal of Geophysical Research B, Solid Earth and Planets 102 (10), 22,815–22,838.

van Heijst, H.J., Snieder, R., Nowack, R., 1994. Resolving a low-velocity zone with surface-wave data. Geophysical Journal International 118, 333–343.

Varentsov, I.M., Engels, M., Korja, T., Smirov, M.Y., BEAR Working Group, 2002. A generalized geoelectric model of Fennoscandia: a challenging database for log-period 3D modelling studies within the electromagnetic array research (BEAR) project. Izvestiya, Physics of the Solid Earth 18 (10), 855–896.

Vidale, J.E., Ding, X.Y., Grand, S.P., 1995. The 410-km-depth discontinuity; a sharpness estimate from near-critical reflections. Geophysical Research Letters 22 (19), 2557–2560.

Villasenor, A., et al., 2001. Shear velocity structure of central Eurasia from inversion of surface wave velocities. Physics of the Earth and Planetary Interiors 123, 169–184.

Walck, M.C., 1984. The P-wave upper mantle structure beneath an active spreading centre; the Gulf of California. Geophysical Journal of the Royal Astronomical Society 76 (3), 697–723.

Warren, D.H., et al., 1968. Project Early Rise Travel Times and Amplitudes. U.S. Geological Surv., Menlo Park, California.

Wyllie, P.J., 1970. Low-velocity zone of the Earth's mantle: incipient melting caused by water. Science 169, 764–766.

Wyllie, P.J., 1995. Experimental petrology of upper mantle materials, processes and products. In: Ribeiro Fernando, B. (Ed.), Proceedings of the International Symposium on the Physics and Chemistry of the Upper Mantle (ISUM). Journal of Geodynamics. Pergamon Press, Oxford, New York, International, pp. 429–468.

Wyllie, P.J., Baker, M.B., White, B.S., 1990. Experimental boundaries for the origin and evolution of carbonatites. In: Woolley, A.R., Ross, M. (Eds.), Alkaline Igneous Rocks and Carbonatites. Lithos. Elsevier, Amsterdam, International, pp. 3–19.

Zhang, Y.S., Tanimoto, T., 1993. High-resolution global upper mantle structure and plate tectonics. Journal of Geophysical Research 98 (6), 9793–9823.